Published online 22 May 2023

Nucleic Acids Research, 2023, Vol. 51, No. 12 ***6321–6336***
https://doi.org/10.1093/nar/gkad423

Abasic site–peptide cross-links are blocking lesions repaired by AP endonucleases

Anna V. Yudkina[1,2,*], Nikita A. Bulgakov[1], Daria V. Kim[1,2], Svetlana V. Baranova[1], Alexander A. Ishchenko[3], Murat K. Saparbaev[3], Vladimir V. Koval[1] and Dmitry O. Zharkov[1,2,*]

[1]SB RAS Institute of Chemical Biology and Fundamental Medicine, Novosibirsk 630090, Russia, [2]Department of Natural Sciences, Novosibirsk State University, Novosibirsk 630090, Russia and [3]Groupe "Mechanisms of DNA Repair and Carcinogenesis", Equipe Labellisée LIGUE 2016, CNRS UMR9019, Université Paris-Saclay, Gustave Roussy Cancer Campus, F-94805 Villejuif, France

Received December 20, 2022; Revised April 18, 2023; Editorial Decision May 03, 2023; Accepted May 15, 2023

ABSTRACT

Apurinic/apyrimidinic (AP) sites are abundant DNA lesions arising from spontaneous hydrolysis of the *N*-glycosidic bond and as base excision repair (BER) intermediates. AP sites and their derivatives readily trap DNA-bound proteins, resulting in DNA–protein cross-links. Those are subject to proteolysis but the fate of the resulting AP–peptide cross-links (AP-PXLs) is unclear. Here, we report two *in vitro* models of APPXLs synthesized by cross-linking of DNA glycosylases Fpg and OGG1 to DNA followed by trypsinolysis. The reaction with Fpg produces a 10-mer peptide cross-linked through its N-terminus, while OGG1 yields a 23-mer peptide attached through an internal lysine. Both adducts strongly blocked Klenow fragment, phage RB69 polymerase, *Saccharolobus solfataricus* Dpo4, and African swine fever virus PolX. In the residual lesion bypass, mostly dAMP and dGMP were incorporated by Klenow and RB69 polymerases, while Dpo4 and PolX used primer/template misalignment. Of AP endonucleases involved in BER, *Escherichia coli* endonuclease IV and its yeast homolog Apn1p efficiently hydrolyzed both adducts. In contrast, *E. coli* exonuclease III and human APE1 showed little activity on APPXL substrates. Our data suggest that APPXLs produced by proteolysis of AP site-trapped proteins may be removed by the BER pathway, at least in bacterial and yeast cells.

GRAPHICAL ABSTRACT

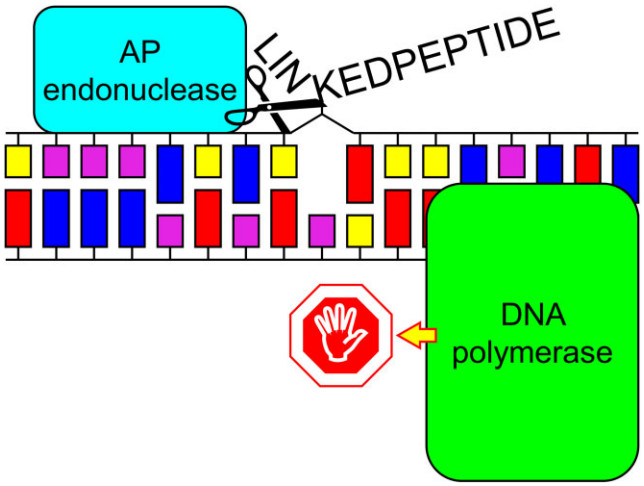

INTRODUCTION

Apurinic/apyrimidinic (AP) sites occur by hydrolysis of the *N*-glycosidic bond in deoxyribonucleotides and are among the most abundant spontaneous and induced DNA lesions in the cell (1,2). They are also formed as intermediates in the base excision repair pathway, often being more genotoxic and mutagenic than the original lesion and thus requiring tight control over their processing (3,4). Chemically, AP sites are a family of lesions, which includes the much-studied aldehydic AP site as well as its derivatives oxidized at C1′ (deoxyribolactone, DRL) (5–7), C2′ (C2-AP) (8), C4′ (C4-AP) or C5′ position (5′-(2-phosphoryl-1,4-dioxobutane), DOB) (9,10).

Normally, AP sites are quickly removed from the genome by the base excision DNA repair (BER) system. However,

*To whom correspondence should be addressed. Tel: +7 383 363 5187; Fax: +7 383 363 5128; Email: dzharkov@niboch.nsc.ru
Correspondence may also be addressed to Anna V. Yudkina. Tel: +7 383 363 5188; Fax: +7 383 363 5128; Email: ayudkina@niboch.nsc.ru

there are important differences in the processing of different types of AP sites. The repair of aldehydic AP sites follows the classical short-patch BER branch, which, in human cells, involves the AP endonuclease (APE1) followed by polymerase and deoxyribophosphate lyase (dRPase) activities of DNA polymerase β (POLβ) (11). At the same time, C2-AP is not a substrate for the dRPase activity of POLβ and is removed through the long-patch branch of BER: the DNA flap containing the lesion at the 5′-end is displaced during the repair DNA synthesis and hydrolyzed by FEN1 nuclease (8,12). DRL repair is even more problematic: this lesion forms DNA–protein cross-links (DPXLs) with Lys residues in the active sites of DNA glycosylase Nth and POLβ (13,14), and the β-elimination product of DRL can similarly trap DNA glycosylases Fpg and NEIL1 (14). The presence of a 1,4-dicarbonyl moiety in C4-AP and DOB also promotes covalent capture of POLβ and DNA polymerase λ (15,16). The irreversible inhibition of the main DNA repair enzymes leads to significant cytotoxicity of modified AP sites (7).

Both aldehydic and oxidized AP sites readily form DPXLs. The covalent capture of many DNA-binding proteins by AP sites has been reported, including histones (6,17,18), integrase (19), DNA ligase (20), Ku antigen (21), as well as RNA-binding proteins (22,23), chaperones (22) and enzymes of carbohydrate metabolism (22,24). Recently, a unique mechanism for the repair of AP sites in single-stranded DNA was discovered (25–27), based on the formation of cross-links between the AP site and the HMCES protein (in human cells) or YedK protein (in *E. coli*), followed by switching to the proteasome-dependent pathway of DPXL repair. Thus, DPXL with AP sites are highly relevant adducts *in vivo*.

DPXLs are not limited to cross-links with AP sites and appear through a multitude of mechanisms including reactions with aldehydes and heavy metals, UV and ionizing radiation, and failed action of enzymes such as topoisomerases or C5-methyltransferases (28,29). Thus, a special pathway dedicated to DPXL repair has evolved. It is tightly coupled to replication and involves proteolytic degradation of the protein part of the cross-link (30–33). However, at the moment it remains poorly understood how the last peptide remnant conjugated with DNA is finally removed. It was suggested that this role can be played by nucleotide excision repair (NER), which normally protects the genome from bulky adducts (34–38). Also, Fpg/Nei-like DNA glycosylases are able to excise oxidized purine residues cross-linked to peptides (38). Recombination repair does not appear to be involved in the removal of peptide conjugates from DNA, although it may play a role in tolerance to larger DPXLs (31,36). It should be noted that all these data were obtained on cross-links chemically different from those formed by AP sites, and peptide adducts of this type remain uncharacterized with respect to their repair and their effect on replication. While the studied peptide adducts with nucleobases usually retain some base-pairing ability, the bulky nature and non-instructing properties of AP site–peptide cross-links make these lesions more problematic for the cell. Here we report a model of stable, chemically determined AP site–peptide cross-links (APPXLs), conjugated through either a terminal or an internal position in the peptide, and show that they block DNA polymerases and can be repaired by AP endonucleases.

MATERIALS AND METHODS

Oligonucleotides and enzymes

Escherichia coli formamidopyrimidine–DNA glycosylase (Fpg) (39), endonuclease VIII (Nei) (40) and endonuclease IV (Nfo) (41), human AP endonuclease (APE1) (42), 8-oxoguanine–DNA glycosylase (OGG1) (43), endonuclease VIII-like protein 1 (NEIL1) (44) and endonuclease VIII-like protein 2 (NEIL2) (45), yeast AP endonuclease (Apn1p) (41), 3′→5′-exonuclease-deficient (exo$^-$) Klenow fragment of *E. coli* DNA polymerase I (KF) (46) and exo$^-$ bacteriophage RB69 DNA polymerase (RBpol) (47) were overexpressed and purified essentially as described. Cloning and purification of DNA polymerase X from African swine fever virus (ASFV PolX) is described below. *E. coli* exonuclease III (Xth) was purchased from Roche (Basel, Switzerland), *E. coli* uracil–DNA glycosylase (Ung) and exonuclease-proficient KF, from SibEnzyme (Novosibirsk, Russia), full-length *E. coli* DNA polymerase I (Pol I) and *Saccharolobus (Sulfolobus) solfataricus* DNA polymerase IV (Dpo4), from New England Biolabs (Ipswich, MA) and trypsin, from Samson-Med (St. Petersburg, Russia). Purity of the DNA polymerases and AP endonucleases, except for those obtained commercially, is illustrated in Supplementary Figure S1. Oligonucleotides (Supplementary Table S1) were synthesized in-house from commercially available phosphoramidites (Glen Research, Sterling, VA).

ASFV PolX cloning and purification

The coding frame of PolX optimized for expression in *E. coli* was synthesized by Gene Universal (Newark, DE, USA) and confirmed by Sanger sequencing. The insert was subcloned into the pET-24b vector (Merck, Darmstadt, Germany) at NdeI/XhoI sites. The plasmid was subsequently introduced into the *E. coli* Rossetta 2(DE3) strain (Merck). One liter of LB medium supplemented with 100 μg/ml of kanamycin was inoculated with 5 ml of an overnight culture. The cells were grown with vigorous shaking at 37°C to A_{600} = 0.6, isopropyl-β-D-thiogalactopyranoside was added to 1 mM, and the growth was continued for 4 h at 37°C. The cells were harvested by centrifugation at 12 000 × g at 4°C for 20 min and stored at –72°C. Before the purification, the pellet was thawed on ice in 40 ml of Buffer A consisting of 20 mM sodium phosphate (pH 7.5), 1 mM ethylenediaminetetraacetic acid (EDTA), 1 mM dithiothreitol (DTT) and supplemented with 500 mM NaCl and 1 mM phenylmethylsulfonyl fluoride. The cells were sonicated, and the lysate was clarified by centrifugation at 12 000 × g at 4°C for 30 min. The supernatant was filtered through a 0.45-μm polyvinylidene difluoride membrane, diluted with four volumes of Buffer A and loaded onto a 5-ml SP Sepharose HiTrap column (GE Healthcare, Chicago, IL) equilibrated in Buffer A plus 100 mM NaCl. The column was washed with Buffer A supplemented with 100 mM NaCl, and PolX was eluted with a NaCl gradient at ∼650 mM. The fractions containing PolX were pooled, diluted with six volumes of Buffer A and loaded onto a

5-ml heparine Sepharose HiTrap column (GE Healthcare) equilibrated in Buffer A plus 100 mM NaCl. The column was washed with the same buffer, and PolX was eluted with a NaCl gradient at ∼730 mM. The fractions containing PolX were pooled, diluted with six volumes of Buffer A and additionally purified on a 1-ml MonoS column (GE Healthcare) previously equilibrated in Buffer A plus 100 mM NaCl. PolX was eluted with a NaCl gradient at ∼600 mM. The fractions containing >90% homogeneous protein were pooled, dialyzed against the buffer containing 20 mM sodium phosphate (pH 7.5), 400 mM NaCl, 1 mM EDTA, 1 mM DTT, and 50% glycerol, and stored at −20°C.

Synthesis of model peptide conjugates with AP sites

DNA cross-links to Fpg or OGG1 proteins were obtained as described (48–50). Briefly, ∼2 nmol of the oligonucleotide duplex (40oG//28down or 28oG//21comp; Supplementary Table S1) was treated with 3–6 nmol of the enzyme in 50 mM sodium phosphate (pH 6.8), 1 mM EDTA, 1 mM DTT and 100 mM $NaBH_4$ in a total volume of 40 μl. The reaction was allowed to proceed at 37°C for 2 h. The resulting DPXL was denatured at 95°C for 10 min, cooled, and pH of the solution was adjusted to ∼8.0 by adding Tris base. The mixture was supplemented with 2 μg of trypsin and incubated for 4 h at 37°C. The oligonucleotide–peptide conjugate was separated by electrophoresis in 20% polyacrylamide/7 M urea, excised under UV illumination, desalted by reverse-phase chromatography on Isolute C18 sorbent (Biotage, Uppsala, Sweden) and characterized by MALDI MS. If necessary, the oligonucleotides for the following experiments were 5′-labeled using γ[^{32}P]ATP and annealed to a 1.5-fold molar excess of the complementary strand.

DNA polymerase assays

For the standing-start assay, the substrates were assembled from the 40-mer template strand containing an APPXL and the ^{32}P-labeled primer (13pri; Supplementary Table S1) or the 28-mer template strand containing an APPXL and the ^{32}P-labeled primer (16pri; Supplementary Table S1). The reaction mixture (10 μl) contained 20 nM pre-annealed substrate, DNA polymerase (100 nM KF or RBpol, 400 nM PolX, 0.1 U/μl Dpo4), dNTPs (either 200 μM individual dATP, dCTP, dGTP, or dTTP, or a mixture of all four dNTPs each at 200 μM) in the reaction buffer (50 mM Tris–HCl (pH 7.5), 5 mM $MgCl_2$ and 1 mM DTT for KF, RBpol and PolX; 20 mM Tris–HCl (pH 8.8), 10 mM $(NH_4)_2SO_4$, 10 mM KCl, 2 mM $MgSO_4$, 0.1% Triton X-100 for Dpo4). The reaction was allowed to proceed at 37°C for 30 min, quenched with an equal volume of the loading solution (80% formamide, 20 mM Na-EDTA, 0.1% xylene cyanol, 0.1% bromophenol blue), and heated for 1 min at 95°C. The reaction products were resolved by 20% denaturing PAGE and visualized on a Typhoon FLA 9500 imager (GE Healthcare). The bands were quantified using Quantity One v4.6.8 (Bio-Rad Laboratories, Hercules, CA). For the running-start assay, the substrates were assembled from the 40-mer template strand containing an APPXL and the ^{32}P-labeled primer (11pri; Supplementary Table S1). The substrates were taken at 50 nM, and the enzymes, at 50 nM (KF or RBpol), 200 nM (PolX) or 0.1 U/μl (Dpo4); aliquots were taken at 2, 5 and 30 min; otherwise the reactions were run and processed as above.

AP endonuclease assay

The substrates were assembled from the ^{32}P-labeled 40-mer strand containing an APPXL and the complementary 40-mer strand (40compC; Supplementary Table S1). The reaction mixture (10 μl) contained 50 nM substrate prepared as above and 10–1000 nM Xth, APE1, Apn1p or Nfo in the respective buffer optimal for BER or NIR (Supplementary Table S2). As a control, instead of the APPXL, we used the same oligonucleotide construct with an aldehydic AP site, freshly prepared by treatment of the U-containing substrate with Ung at 37°C for 20 min. The endonuclease reaction was allowed to proceed at 37°C for 30 min, treated and analyzed as above.

AP endonuclease kinetics

The reaction mixture (10 μl) contained increasing concentrations of the ^{32}P-labeled 40-mer APPXL substrates or control substrates 23OHU:23comp or 20THF:20comp (1–500 nM) in the BER or NIR buffer. Concentrations of AP endonucleases were optimized for each substrate and buffer to produce ≤20% cleavage and were in the 5 pM–0.5 nM range. The reaction was allowed to proceed for 10 min at 37°C, treated and analyzed as above. The data were fitted by nonlinear regression to the Michaelis–Menten equation using Sigmaplot v11.0 (Systat Software, Chicago, IL). The reported values are averages of 3–5 independent experiments.

AP endonuclease / DNA polymerase assay

The reaction mixture (10 μl) contained 200 nM ^{32}P-labeled duplex 40-mer APPXL substrate and 50–150 nM Nfo in the BER buffer (Supplementary Table S2). After 10 min, the reaction mixture was supplemented with dNTPs (200 μM each), 5 mM $MgCl_2$ and 50–250 nM KF. The reaction was allowed to procced at 37°C for 2, 5 or 30 min, treated and analyzed as above.

DNA glycosylase assay

The reaction mixture (10 μl) contained 10 nM labeled duplex substrate (see above), 1 μM DNA glycosylase (*E. coli* Fpg or Nei, human OGG1, NEIL1 or NEIL2), 50 mM Tris–HCl (pH 7.5), 100 mM NaCl, 1 mM EDTA and 1 mM DTT. The reaction was allowed to proceed at 37°C for 30 min, treated and analyzed as above.

RESULTS

Synthesis and characterization of DNA–peptide cross-links with AP site

Since AP sites can form cross-links to a variety of proteins, which can be further processed to APPXLs, it is usually assumed that the repair of such adducts does not depend on the exact nature of the cross-linked peptide. Hence, to obtain model APPXLs, we made use of two

enzymes, *E. coli* Fpg and human OGG1 DNA glycosylases, that form transient covalent intermediates with AP sites during the catalysis. To excise the damaged base (8-oxoguanine; 8-oxoG) from DNA, Fpg and OGG1 carry out a nucleophilic attack by an amino group at the C1′ atom of the target nucleotide forming a labile Schiff base, which may be nearly quantitatively reduced by $NaBH_4$ or $NaBH_3CN$ to a stable conjugate (Figure 1). This reaction was successfully used to crystallize covalent Fpg–DNA and OGG1–DNA complexes (39,51) and to study the interaction of full-length DPXLs with the replication and repair machinery (36,48–50). Thus, we first prepared DPXLs by treatment of 8-oxoG-containing duplexes with Fpg or OGG1 in the presence of $NaBH_4$ and subjected them to trypsinolysis (Supplementary Figure S2A, B). Fpg and OGG1 belong to different structural superfamilies and use different nucleophilic residues for catalysis: N-terminal Pro1 in Fpg and Lys249 in OGG1. Hence, after trypsinolysis, the resulting peptide conjugates are expected to have different structures (Figure 1). The Fpg–DNA conjugate gives an adduct with the decapeptide (P)ELPEVETSR (the residue that forms the cross-link is in parentheses), in which the peptide forms a bond with DNA through its N-terminus. On the other hand, trypsinolysis of the OGG1 conjugate should give an adduct with the 23-mer peptide ALCILPGVGT(K)VADCICLMALDK, cross-linked trough an internal position of the peptide. Based on the visual resemblance (Figure 1), we will further call these AP site–peptide cross-links APPXL-I (terminally adducted, linear peptide) and APPXL-Y (an adduct trough an internal residue with two peptide branches).

APPXL-I and APPXL-Y were purified by denaturing polyacrylamide gel electrophoresis followed by reverse-phase chromatography and characterized by MALDI-TOF mass spectrometry (Supplementary Figure S2C, D). The yield of the homogeneous stable APPXLs was ∼5–15% of the initial 8-oxoG-containing oligonucleotide. In addition to the cross-link with the full-length modified strand, we have observed some products that likely corresponded to products of strand cleavage by Fpg/OGG1, which were easily separated from the major adduct by electrophoresis (Supplementary Figure S2A, B). Despite the long oligonucleotide parts, of the cross-links, their masses were better resolved by MALDI mass spectrometry in a positive mode and were within a few Da of the expected values. No peaks of the starting material (expected [M + H^+], 12138.9 Da) was evident, indicating good separation of the APPXLs by electrophoresis. In the APPXL-I mass spectrum, we observed two peaks corresponding to the expected molecular weight of the adduct of the 40-mer oligonucleotide with the (P)ELPEVETSR peptide (observed [M + H^+], 13131.0 Da, expected, 13127.9 Da) and (P)ELPEVETSRR peptide (observed [M + H^+], 13285.8 Da, expected, 13284.0 Da), most likely resulting from incomplete trypsin cleavage at two adjacent Arg residues (Supplementary Figure S2C). As heterogeneity of cross-linked peptides may be naturally expected from proteolysis of DPXLs in the cell, we have proceeded to characterize the biochemical properties of our adducts.

AP site–peptide cross-links block DNA polymerases

To investigate the ability of DNA polymerases to bypass APPXLs, we annealed the cross-linked template oligonucleotide with a labeled primer with its 3′-terminus placed 12 bases upstream of the cross-link site (‘running start’ conditions, see the substrate schemes in Figures 2A, B, 3A). This distance exceeds the footprints of the full-length proteins from which the cross-linked peptides were derived, and thus the peptide was not expected to prevent DNA polymerase binding. We also tested the ability of DNA polymerases to carry out synthesis through the APPXL in the context of DNA duplex when the polymerase has to displace the downstream strand (Figures 2C, D, 3B). As APPXLs are non-instructive, both APPXL-I and APPXL-Y are expected to be strongly blocking. Therefore, we used a natural freshly prepared AP site as a control to determine which events would result from DNA polymerases blocking due to the lack of a base or due to the nature of cross-linked peptide. Non-damaged primer–template or primer–downstream strand–template constructs were used as polymerase activity controls.

Four DNA polymerases, representing a range of structural and functional features, were investigated. As we were interested in the general ability of DNA polymerases to bypass APPXLs, we opted to use easily accessible representative members of various structural families originating from bacteria, archaea, and viruses, rather than human enzymes. The Klenow fragment of *E. coli* DNA polymerase I (KF) belongs to Family A of DNA polymerases, acting in DNA repair and replication. The homologous human enzymes are DNA polymerases γ, θ and ν. Bacteriophage RB69 DNA polymerase (RBpol) is a high-fidelity replicative polymerase from Family B and is often taken as a convenient model of structurally related human replicative DNA polymerases α, δ and ε, and a translesion DNA polymerase ζ. In both cases, we have used 3′→5′-exonuclease-deficient versions of the polymerases to prevent primer degradation; exonuclease-proficient KF was also brought in for comparison. DNA polymerase X (PolX) from African swine fever virus (ASFV) belongs to structural Family X, mostly engaged in DNA repair and encompassing human DNA polymerases β, λ, and μ. Finally, DNA polymerase IV from *Saccharolobus* (formerly *Sulfolobus*) *solfataricus* (Dpo4) is a representative of Family Y translesion polymerases, of which human cells possess DNA polymerases η, ι and κ.

Under the running start conditions, the blocking properties of APPXL-I were comparable with the properties of the natural AP site: KF demonstrated slightly better bypass of APPXL-I compared to AP site in comparison with RBpol, which was slightly more efficient on AP site-containing substrates. After 30 min, KF was able to fully elongate 6.8% of the primer if APPXL-I was in the template, and only 4.6% if an AP site was in the template whereas RB69 demonstrated 6.6% bypass of APPXL-I and 11% of the AP site (Figure 2A). Moreover, two strong pause points were evident one nucleotide before the cross-linking site and directly opposite the cross-link (23- and 24-nt long products; marked by

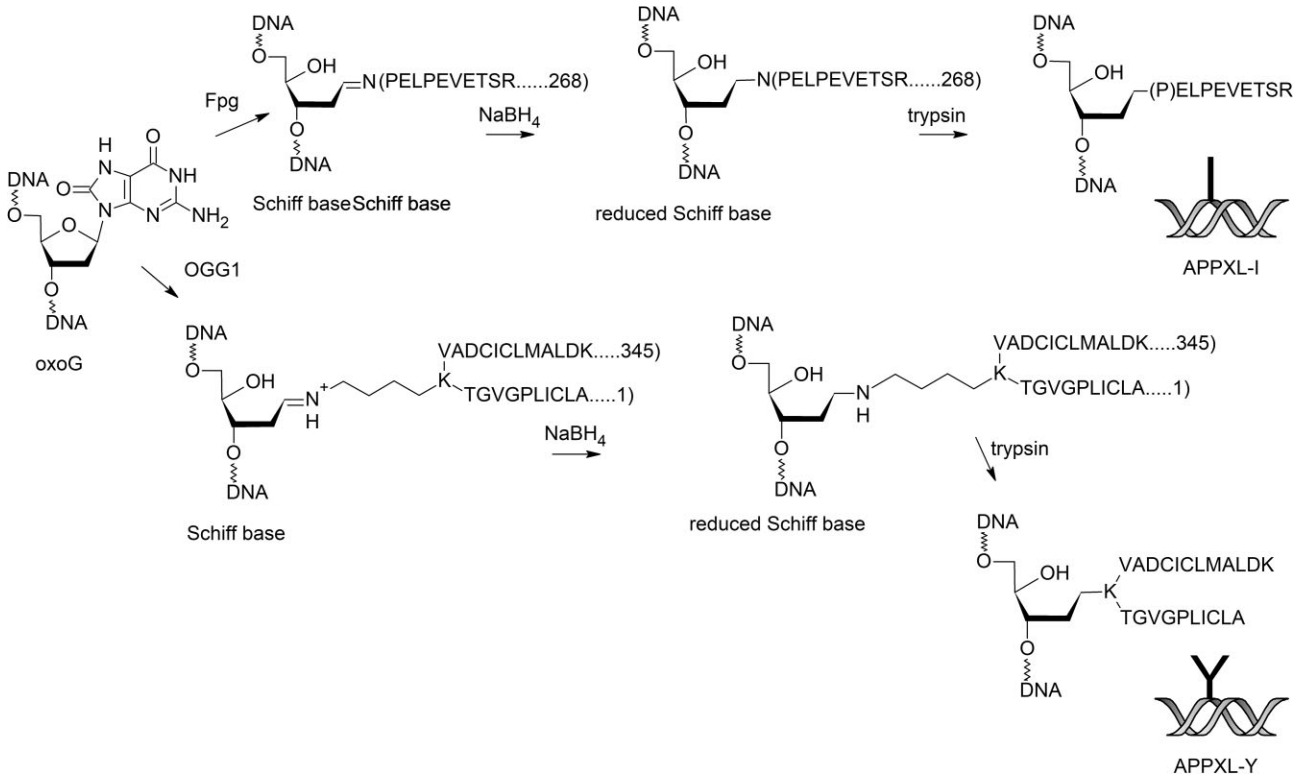

Figure 1. Scheme of the DNA–peptide cross-link preparation. 8-OxoG-containing DNA duplexes were treated with bifunctional DNA glycosylases Fpg (top) or OGG1 (bottom) to produce a Schiff base conjugate with the nascent aldehydic AP site through a terminal amino group in case of Fpg or an internal amino group in case of OGG1. The enzyme–DNA intermediates were stabilized with $NaBH_4$ to yield covalent DNA–protein cross-links (DPXLs). Then, DPXL were subjected to full trypsinolysis to obtain AP–peptide cross-links.

grey arrows in Figures 2 and 3), indicating low ability of DNA polymerases both to incorporate a dNMP opposite APPXL-I and to extend the primer after such incorporation. The absence of any additional pause points suggests that the bulky peptide does not hamper moving DNA polymerase access to the cross-link site. The aldehyde AP site produced a single pause point one nucleotide before the lesion. Exonuclease-proficient KF demonstrated the same behavior as KF exo$^-$ except for noticeable primer degradation at longer reaction times (Supplementary Figure S3). Thus, APPXL-I, while strongly blocking, still allows better incorporation of a dNMP than the smaller non-instructive AP site. PolX, which is known to be nearly fully blocked by AP sites (52), demonstrated no bypass of the APPXL-I as well as the natural AP site, showing a single pause point corresponding to the 23-mer synthesis product (Figure 3A). Blocking of PolX may be due to its distributive mode of synthesis, which facilitates DNA release and complicates polymerase binding near the blocking lesion. Translesion DNA polymerase Dpo4, as expected, demonstrated the strongest ability to bypass the AP site (Dpo4 was able to fully elongate ∼28% of the primer) and APPXL-I (∼30% of the bypass), producing the same two pause points in the latter case (Figure 3A). The presence of a downstream strand complicated the bypass of the blocking lesion, yet the synthesis pause points and the relative efficiency of lesion bypass seen with the primer–template system were preserved (Figures 2C, 3B).

Strong polymerase inhibition and two pronounced pause points for KF, RBpol and Dpo4 were also evident for substrates containing the branched APPXL-Y adduct (Figures 2B, D, 3, Supplementary Figure S3). The bulkier APPXL-Y turned out to be even more blocking than APPXL-I. The pause point corresponding to the 24-nt product for KF and RBpol was weaker than the corresponding pause for APPXL-I, and the full-length product decreased significantly for KF and Dpo4.

We have also addressed polymerase-blocking ability of AP site–peptide cross-links present in an internal position of the non-template downstream strand. However, only for PolX was a minor pause point observed, while KF and RBpol displaced the cross-linked strand without effort, and Dpo4, while having lower strand displacement activity, did not pause at the cross-link (Supplementary Figure S4).

Interestingly, when different substrates were compared, we systematically observed primer utilization efficiency decreasing in the order AP site >APPXL-I > APPXL-Y. Possibly, the peptide part may partially interfere with DNA binding by the polymerase even when the primer end is 12 nt away from the cross-link site, for example, by obstructing non-specific DNA binding and facilitated diffusion used by polymerases to locate the primer end (53). The only exception was Dpo4 with APPXL-Y in the downstream strand, in which case the bulky peptide adduct might destabilize the duplex and improve the poor strand displacement ability of Dpo4.

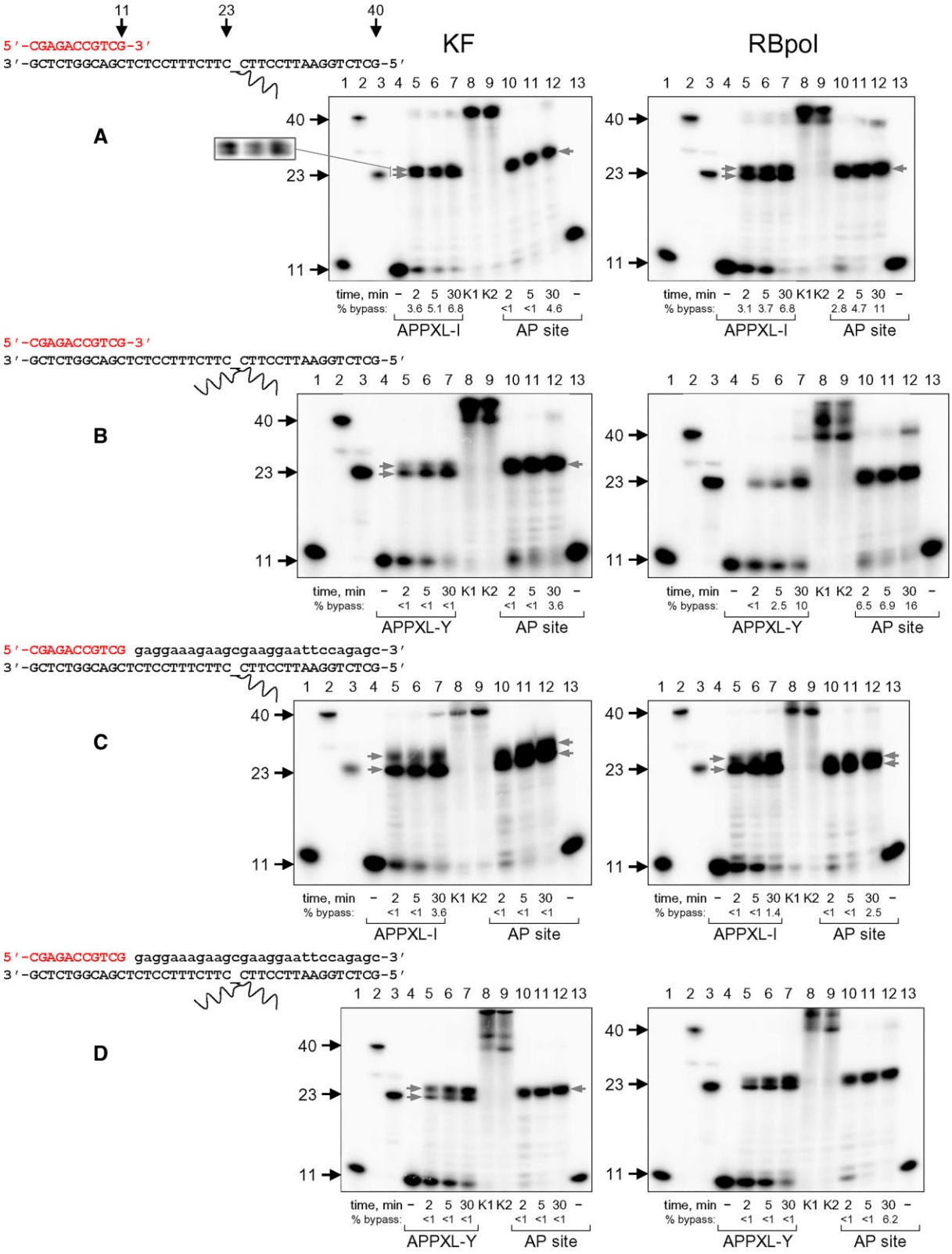

Figure 2. Stalling of KF and RBpol by AP–peptide cross-links. (**A**) APPXL-I, primer–template; (**B**) APPXL-Y, primer–template; (**C**) APPXL-I, primer–downstream strand–template; (**D**) APPXL-Y, primer–downstream strand–template. The ^{32}P-labeled primer is shown in red, the downstream strand is in lowercase. Grey arrows mark the sites of synthesis termination at the lesion. Reaction time and the nature of the lesion are indicated under the gel images. In all panels, lanes 1–3 are size markers corresponding to the primer (11 nt), full-size product (40 nt), and primer extended to the cross-link site (23 nt). "–", no enzyme added; K1, undamaged primer–template, 30 min; K2, undamaged primer–template–downstream strand, 30 min. The inset shows KF pause sites at a lower band intensity.

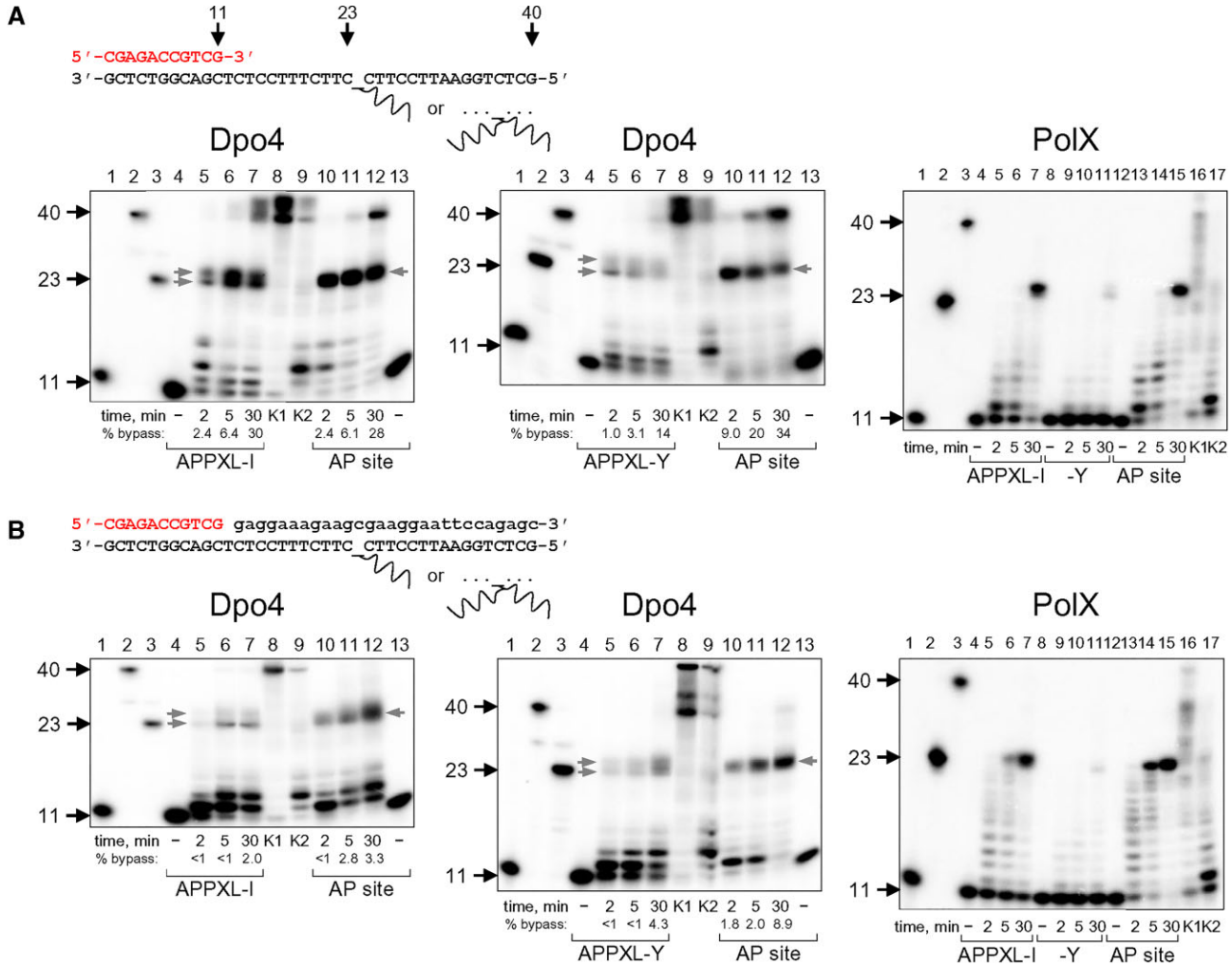

Figure 3. Stalling of Dpo4 and PolX by AP–peptide cross-links. (**A**) Primer–template; (**B**) primer–downstream strand–template. The nature of the polymerase and the cross-link is indicated over and below the gel images, respectively. The ^{32}P-labeled primer is shown in red, the downstream strand is in lowercase. Grey arrows mark the sites of synthesis termination at the lesion. Reaction time and the nature of the lesion are indicated under the gel images. In all panels, lanes 1–3 are size markers corresponding to the primer (11 nt), full-size product (40 nt) and primer extended to the cross-link site (23 nt). "–", no enzyme added; K1, undamaged primer–template, 30 min; K2, undamaged primer–template–downstream strand, 30 min. No bypass was observed for PolX.

AP site–peptide cross-links mostly direct A and G incorporation and can induce primer–template misalignment

Since we observed some dNMP insertion opposite APPXLs, we sought to explore the spectra of the incorporated nucleotides. To do this, we moved the primer to place its 3′-end immediately next to the site of the lesion and presented the polymerases with the individual dNMPs as well as with their mixture ('standing start' conditions, Figure 4). Here, KF utilized the APPXL-I adducted template much better than the APPXL-Y adduct, whereas for RBpol the efficiency was somewhat better for the APPXL-Y. Notably, in all cases the primer elongation was significantly lower than under the running start conditions, most likely because the bulky peptide interferes with DNA polymerases' binding to the primer/template junction. Nevertheless, the polymerase preferences for dNMP incorporation opposite APPXLs were clear. Both KF and RBpol predominantly incorporated dAMP, and, to a lesser extent, dGMP (Figure 4A, B). We observed the preference of dNMP incorporation in the order A > G > C > T, which is consistent with the 'A rule', the preference pattern for better dAMP incorporation opposite the AP site (54–56). dGMP incorporation could possibly be explained by template/primer slippage since the next base after the lesion in the template is C. To address this possibility, we repeated the experiment with the substrate of another sequence featuring G as the next base (Supplementary Figure S5), for which template/primer slippage would guide the incorporation of dCMP. However, the same general dNMP incorporation pattern A > G > C > T for KF and RBpol was observed (Supplementary Figure S5A, S5B), confirming that these preferences characterize the miscoding properties of the peptide adducts rather than the tendency for template misalignment. The order of preference of dNTP incorporation by the Family Y Dpo4 was G >> A > C,T (Figure 4C); however, when the substrate was switched, the preference for dNTP usage changed completely to C >> A > G,T (Supplementary Figure S5C), in-

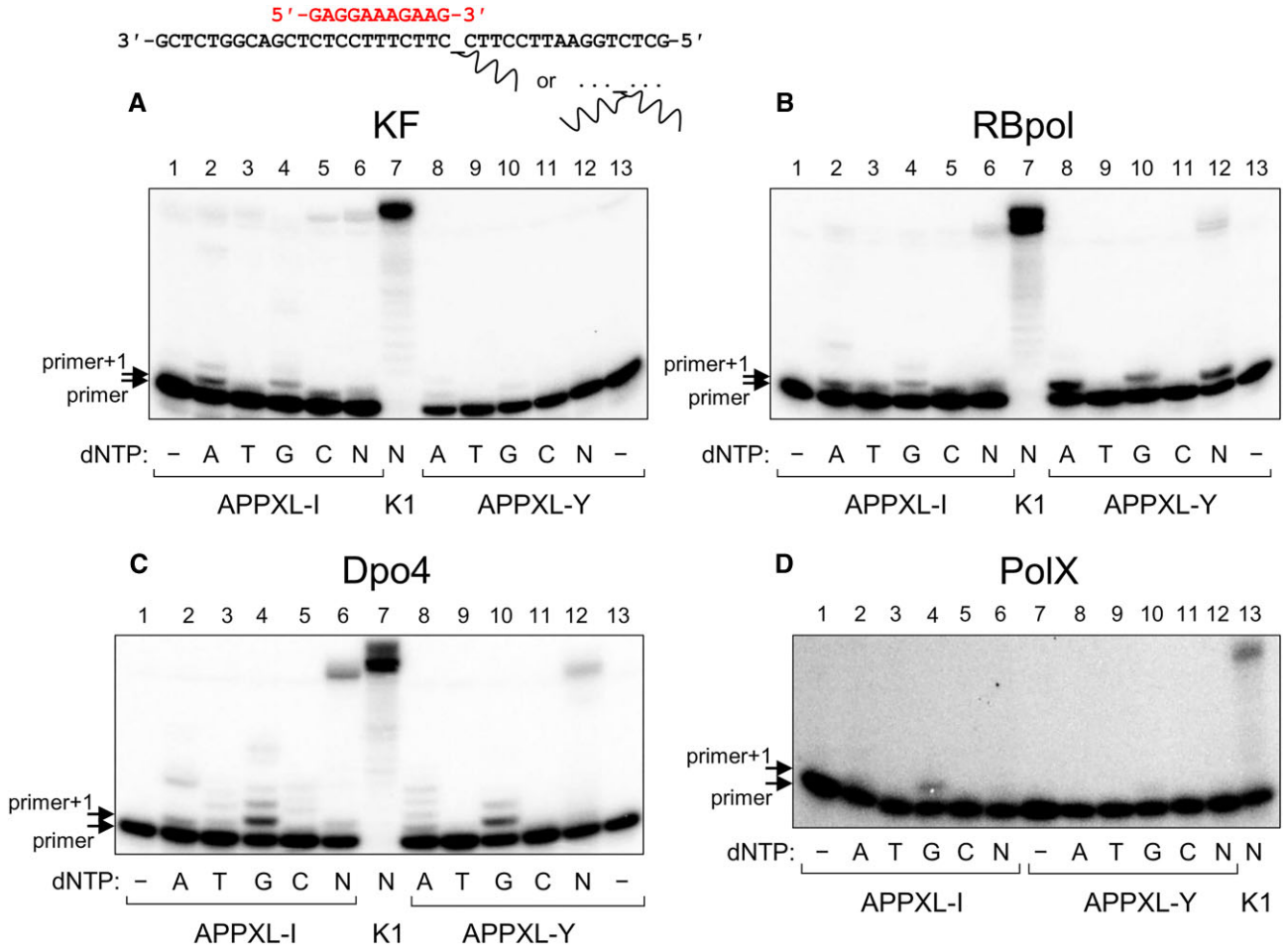

Figure 4. Incorporation of dNMPs opposite APPXLs by KF (**A**), RBpol (**B**), Dpo4 (**C**) and PolX (**D**). The nature of the substrate and dNTP is indicated below the gel images. The ^{32}P-labeled primer is shown in red. '–', no enzyme or dNTPs added; N, all dNTPs added; K1, undamaged primer–template, all dNTPs, 30 min.

dicating that Dpo4 use + 1 nucleotide template misalignment mechanism rather than the 'A rule' during the synthesis on the AP–peptide APPXL-containing substrates. Dpo4 tended to misincorporate several nucleotides, in agreement with its reported low fidelity characteristic of Family Y DNA polymerases (57). PolX also bypassed the peptide adduct by + 1 slippage mechanism, albeit with a low efficiency: the enzyme preferred G > A, T, C on the substrate presenting C as the +1 template nucleotide while changing the specificity to C > A >> T, G on the substrate presenting G at this position (Figure 4D, Supplementary Figure 5D).

AP site–peptide cross-links can be processed by AP endonucleases

Aldehydic AP sites and many of their natural and synthetic modifications are removed from DNA through the BER pathway initiated by AP endonucleases. These enzymes belong to two major unrelated structural groups: the exonuclease–endonuclease–phosphatase (EEP) superfamily and the triosephosphate isomerase (TIM) barrel superfamily. Therefore, we have tested representative members of each group—*E. coli* exonuclease III (Xth) and the main human AP endo/exonuclease 1 (APE1) from the EEP superfamily and *E. coli* endonuclease IV (Nfo) and yeast endonuclease Apn1p from the TIM barrel superfamily—for their ability to cleave oligonucleotide substrates containing APPXL-I or APPXL-Y. Notably, all these enzymes but Xth, in addition to their AP endonuclease activity, were shown to possess the 'nucleotide incision repair' (NIR) activity that cleaves DNA 5′ to many lesions of different chemical nature including quite bulky ones such as 1,N^6-etheno-dA, 3,N^4-etheno-dC, and 3,N^4-benzetheno-dC (41,58–62). Since the pH, buffer and ionic composition optimal for BER and NIR are enzyme-specific, we tested the ability of these AP endonucleases to cleave APPXL-containing substrates under both conditions (Supplementary Table S2).

APE1 efficiently hydrolyzed the natural AP site but did not yield any detectable product of the APPXL-I substrate cleavage (Figure 5A). However, the APPXL-Y substrate was modestly hydrolyzed by APE1, especially under NIR conditions (Figure 6A). This result was rather surprising, since the bulkier APPXL-Y adduct was expected to have larger inhibitory effect, and suggested that the chemical nature of the peptide adduct may be important for its

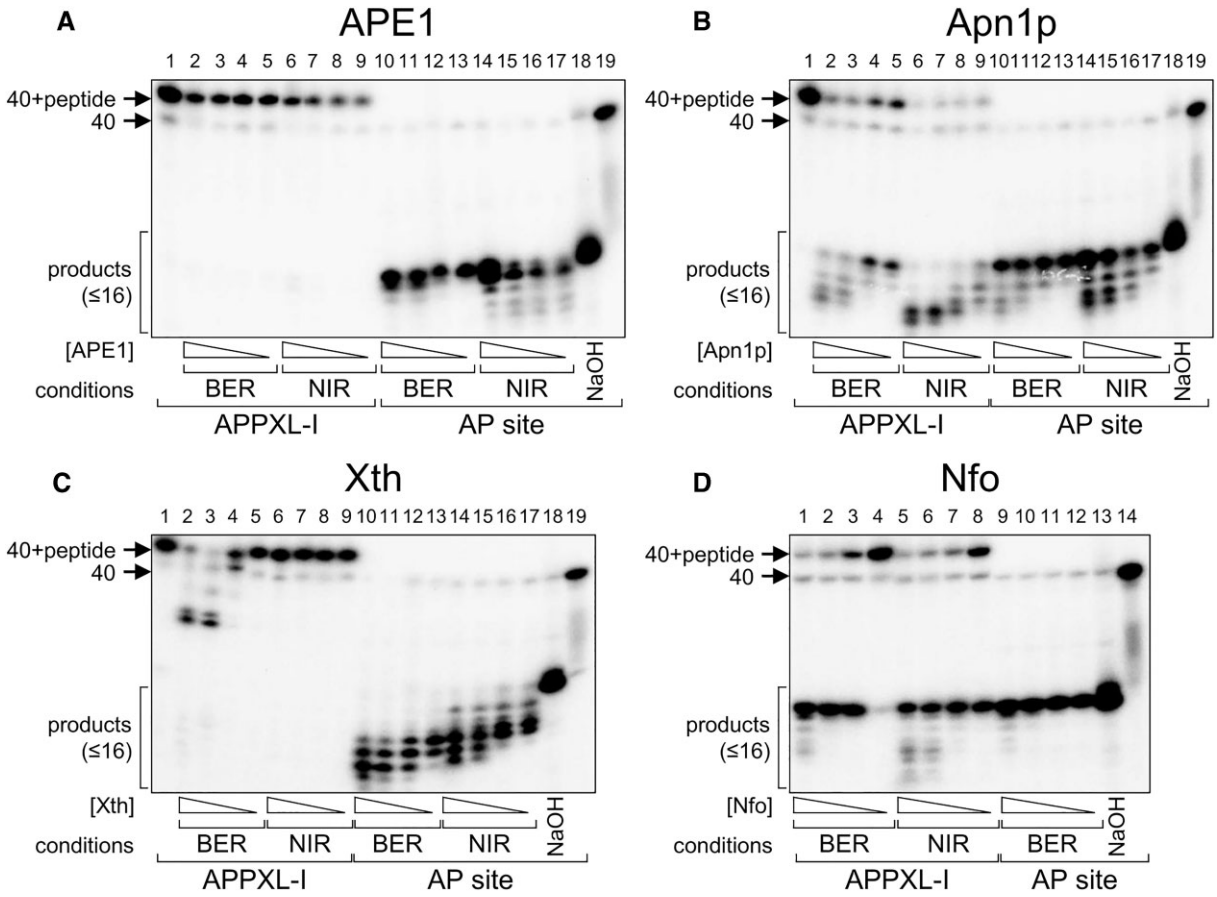

Figure 5. Cleavage of APPXL-I by AP endonucleases: APE1 (**A**), Apn1p (**B**), Xth (**C**) and Nfo (**D**). For panels A–C: lane 1, APPXL-I, no enzyme; lanes 2–5, APPXL-I cleavage under the BER conditions; lanes 6–9, APPXL-I cleavage under the NIR conditions; lanes 10–13, AP site cleavage under the BER conditions; lanes 14–17, AP site cleavage under the NIR conditions; lane 18, AP site treated with NaOH; lane 19, AP site, no enzyme. Panel D: lanes 1–4, APPXL-I cleavage under the BER conditions; lanes 5–8, APPXL-I cleavage under the NIR conditions; lanes 9–12, AP site cleavage under the BER conditions; lane 13, AP site treated with NaOH; lane 14, AP site, no enzyme. BER and NIR conditions for the individual AP endonucleases are specified in Supplementary Table S2.

recognition by AP endonucleases. Another member of the EEP superfamily, Xth, also showed low activity on substrates of both types (Figures 5C, 6C). The degradation product observed at the highest enzyme concentrations migrates slower than the expected APPXL cleavage product and is likely due to the robust 3′→5′-exonuclease activity of Xth evident on the AP substrate. In contrast to APE1 and Xth, both Nfo and Apn1p efficiently processed the substrates containing APPXL-I or APPXL-Y adducts, cleaving the DNA at the cross-link site and showing some additional exonucleolytic degradation (Figures 5B, D, 6B, D). The cleavage was evident under either BER or NIR conditions. Thus, both TIM barrel AP endonucleases cleaved APPXL-containing DNA significantly better than did EEP superfamily AP endonucleases.

To compare the efficiency of AP endonucleases processing APPXLs with their established substrates in a quantitative way, we have measured the steady-state kinetic parameters (K_M, k_{cat}, and the catalytic efficiency k_{cat}/K_M) values using duplex oligonucleotides containing APPXL-I, APPXL-Y, (3-hydroxytetrahydrofuran-2-yl)methyl phosphate (THF, an AP site analog resistant to β-elimination and often used as a model AP site in BER studies) or 5-hydroxy-2′-deoxyuridine (OHU, a typical NIR substrate) (61,62). As shown in Table 1 and Supplementary Figure S6, the apparent k_{cat}/K_M values confirm APPXL-Y is a better substrate compared to APPXL-I for all studied AP endonucleases. For the TIM barrel enzymes, APPXL-Y cleavage activity was comparable with (∼0.5-fold for Apn1p) or even significantly higher than (∼13-fold for Nfo) the OHU cleavage, strongly suggesting that these AP endonucleases may be biologically relevant for processing of AP site–peptide adducts. Moreover, even under BER conditions the efficiency of APPXL-Y cleavage by Nfo was comparable with THF cleavage (THF favored only ∼2-fold). More efficient processing of APPXL-Y than of APPXL-I may also be of biological importance, as peptides covalently bound to the AP site through an internal residue are statistically more likely to arise in the cell after protein conjugation followed by proteolysis.

We also tested the ability of several bifunctional DNA glycosylases capable of AP site cleavage, namely *E. coli* Fpg and Nei, human OGG1, NEIL1 and NEIL2, to cleave the APPXL adducts. However, none of them was able to process cross-links of either type to any significant degree (Supplementary Figure S7).

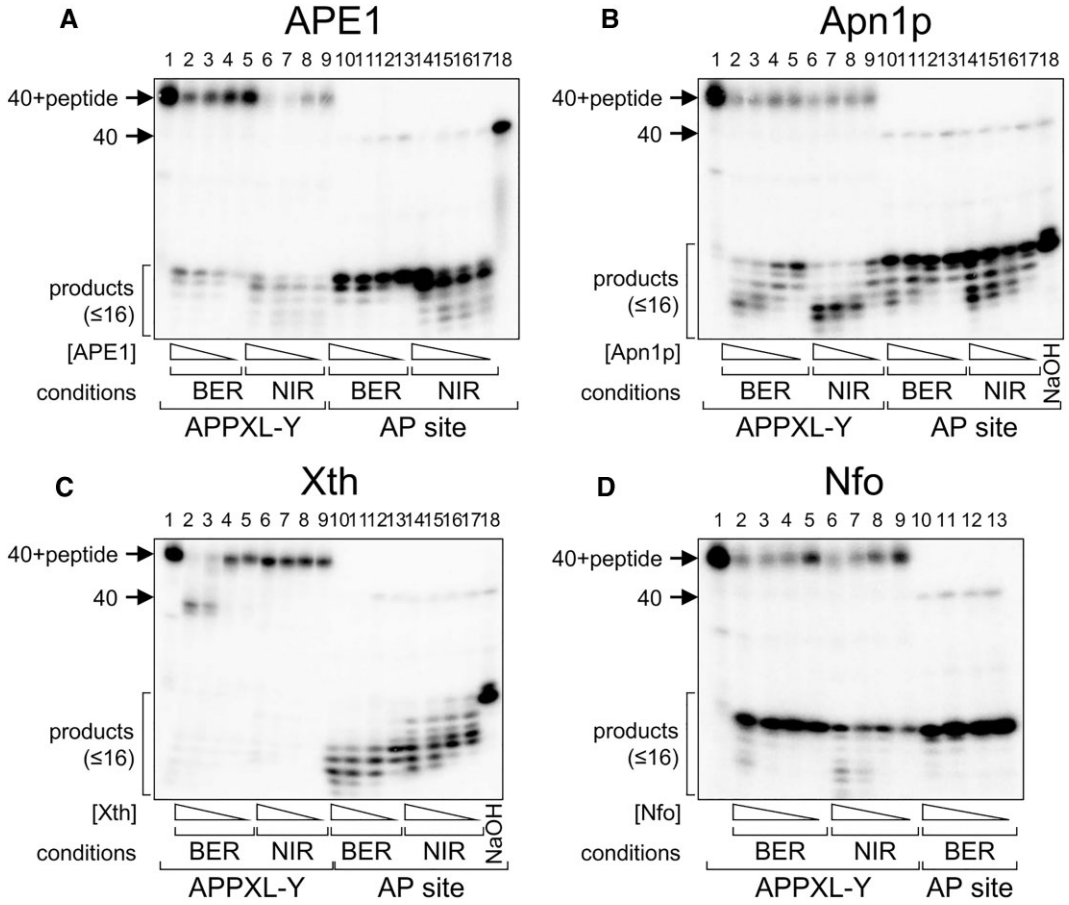

Figure 6. Cleavage of APPXL-Y by AP endonucleases: APE1 (**A**), Apn1p (**B**), Xth (**C**) and Nfo (D). For panels A–C: lane 1, APPXL-Y, no enzyme; lanes 2–5, APPXL-Y cleavage under the BER conditions; lanes 6–9, APPXL-Y cleavage under the NIR conditions; lanes 10–13, AP site cleavage under the BER conditions; lanes 14–17, AP site cleavage under the NIR conditions; lane 18, AP site untreated (A) or treated with NaOH (B, C). Panel D: lane 1, APPXL-Y, no enzyme; lanes 2–5, APPXL-Y cleavage under the BER conditions; lanes 6–9, APPXL-Y cleavage under the NIR conditions; lanes 10–13, AP site cleavage under the BER conditions. BER and NIR conditions for the individual AP endonucleases are specified in Supplementary Table S2.

Strand with a hanging 5′-terminal peptide cross-link can be displaced by DNA polymerases

AP endonucleases nick DNA 5′ of the lesion producing a hanging 5′-terminal 2′-deoxyribophosphate (or another lesion remnant if the substrate was something else than an aldehydic AP site) and a free 3′-OH, which then serves as a primer for a DNA polymerase. To see whether the nick with a 5′-terminal peptide adduct can be processed in the same way, we have first treated the APPXL-I or APPXL-Y substrate with Nfo and then added KF and all four dNTPs (Figure 7A, B). Although in both cases a pause was observed after the incorporation of one nucleotide, eventually the full-length primer extension product was synthesized. Thus, even if the peptide part of the cross-link interferes with polymerase binding or the early steps of primer extension, once the flap is > 1 nt there is apparently no obstacles for further strand displacement.

Furthermore, we have reconstituted the full BER cycle with APPXL-I (annealed opposite to G; 40compG template strand), Nfo, full-length *E. coli* DNA polymerase I, and DNA ligase. Unlike KF, Pol I degrades the strand ahead by a combined exo/endonucleolytic action as it extends the primer (63). To prevent full degradation of the downstream strand, we have omitted dATP and dGTP from the reaction mixture, which should cause the polymerase to stop after incorporating 14 nt, yielding a 30-mer product (Figure 7C). Nfo cleaved the duplex at the adduct, producing the 16-mer with the 3′-OH end, which served as an entry point for Pol I (Figure 7C). In the absence of dNTPs, the 3′→5′ exonuclease activity of Pol I degraded the primer, whereas addition of dCTP and dTTP allowed primer extension to the position of the first pyrimidine in the template. Finally, if DNA ligase was present, the product had a higher electrophoretic mobility than the DNA–peptide adduct, migrating approximately at the same level as an undamaged 40-mer (Figure 7C), which clearly indicated that the repair took place.

These observations support the possibility of APPXL removal via the long-patch BER subpathway (Figure 7D). Obviously, short-patch repair is also possible if a non-stabilized 5′-terminal conjugate can be processed by a dRP lyase.

DISCUSSION

For many years, AP sites were considered a fairly well studied type of DNA damage, but recent discoveries regarding new features of their enzymatic processing and

Table 1. Steady-state kinetics of cleavage of APPXL substrates by AP endonucleases

Enzyme	Substrate	Conditions	K_M (nM)	k_{cat}, s^{-1} ($\times 10^{-5}$)	k_{cat}/K_M, $nM^{-1} \cdot s^{-1}$ ($\times 10^{-8}$)
Apn1p	APPXL-I	BER	190 ± 60	2.0 ± 0.3	10 ± 3
Apn1p	APPXL-I	NIR	21 ± 8	1.2 ± 0.1	58 ± 24
Apn1p	APPXL-Y	BER	110 ± 30	47 ± 5	430 ± 130
Apn1p	APPXL-Y	NIR	200 ± 80	65 ± 13	330 ± 150
Apn1p	THF	BER	8.8 ± 3.0	160 ± 20	18600 ± 6700
Apn1p	OHU	NIR	61 ± 21	38 ± 4	620 ± 220
Nfo	APPXL-I	BER	n/s[a]	n/s	5.2 ± 1.0
Nfo	APPXL-I	NIR	130 ± 50	6.5 ± 1.0	50 ± 20
Nfo	APPXL-Y	BER	n/s	n/s	200 ± 30
Nfo	APPXL-Y	NIR	61 ± 17	260 ± 20	4200 ± 1200
Nfo	THF	BER	150 ± 60.0	66 ± 12	430 ± 180
Nfo	OHU	NIR	140 ± 40.0	46 ± 5	320 ± 90
APE1	APPXL-I	BER	n/c[b]	n/c	n/c
APE1	APPXL-I	NIR	n/c	n/c	n/c
APE1	APPXL-Y	BER	n/c	n/c	n/c
APE1	APPXL-Y	NIR	44 ± 19	1.6 ± 0.2	37 ± 16
APE1	THF	BER	21 ± 7	580 ± 70	28200 ± 10000
APE1	OHU	NIR	170 ± 80	19 ± 4	110 ± 50

[a]n/s, not saturated, saturation with substrate could not be achieved; k_{cat}/K_M determined from the initial phase of reaction velocity *vs* substrate concentration plots.
[b]n/c, not cleaved, cleavage absent or too low to reliably estimate kinetic constants.

biologically relevant reactions of AP sites with non-specific DNA-bound proteins (18,25–27) put these lesions in an unexpected perspective. There is mounting evidence that native and oxidized AP sites in the cell can covalently capture proteins to form highly toxic DNA–protein cross-links. Several breakthrough works in recent years have outlined the general repair scheme for DNA damage of this type. DPXLs mainly serve as substrates for a specialized repair pathway, which is initiated by proteolytic degradation of the protein part of the cross-link by the proteasome or specialized replication-associated proteases (SPRTN1, FAM111A, DDI1, or others yet to be discovered) to a small peptide (30–33). What happens after that, however, remains poorly understood. The studied models of naturally occurring DNA–peptide cross-links include peptide conjugates with exocyclic amino groups of G and A modified through (i) a γ-hydroxypropano bridge (a product of acrolein-induced DNA damage) (35,64–66) or (ii) through a C2 linker derived from alkylation of Cys residues by 1,2-dibromoethane (67) and (iii) conjugates at the aldehyde group of 5-formylcytosine (68–70). In addition, unnatural adducts that are readily obtained synthetically, such as products of azide–alkyl addition to the functionalized C5 position of thymine (71) and cross-links to 7-deaza-7-(2-oxoethyl)guanine (72), were used as model systems.

The major difference between peptide cross-links through nucleobases and through AP sites is the inability of the latter to form complementary bonds. Until now, there have been no reports in the literature regarding the levels of APPXLs, their effect on DNA polymerases or the ways to repair such residual damage. However, recent data on the reactivity of aldehyde and oxidized AP sites suggest that the number of cross-links with the AP site can be comparable to the number of cross-links with bases, or even exceed them. Moreover, some conjugates with oxidized AP sites are much more stable than reversible imine conjugates with aldehydic AP sites. In this work, we developed a model to generate cross-links of AP sites with peptides of different structure based on the reduction of the Schiff base intermediate formed by DNA glycosylases Fpg and OGG1 followed by trypsinolysis. Fpg carries an N-terminal nucleophilic amino group and, after proteolysis, leaves behind a decapeptide attached via its end (APPXL-I), while OGG1 uses the internal Lys249 for catalysis, and upon trypsinolysis yields a longer peptide remnant, in which the cross-link is formed at an internal position (APPXL-Y). This peptide adduct may be of greater biological relevance because DPXLs in the cell are statistically much more likely to be attached within the polypeptide chain, and protease cleavage immediately next to the cross-link point may be hindered by DNA. Although the diversity of proteins capable of cross-linking to DNA dictates the universality of the mechanisms for APPXL repair, the size and properties of the peptide remnant might be expected to affect the APPXL interactions with DNA polymerases and the repair machinery.

A key aspect of APPXL biochemistry determining their biological consequences is the ability to block DNA polymerases or guide incorporation of particular dNMPs. Although no single DNA–peptide adduct was studied with a fully representative set of DNA polymerases, *in vitro* experiments with peptides conjugated through nucleobases show that bypass of such lesions depends both on their size and the preservation of complementarity. DNA polymerases bind DNA in the minor groove and leave the major groove mostly accessible, so bulky moieties occupying the major groove may be better tolerated. For example, 5-formylcytosine adducts or peptides attached to the C5 position of dU through click chemistry, which protrude to the major groove and do not interfere with base pairing, are quite easily bypassed by both replicative and translesion human DNA polymerases, although longer peptides may present a problem (e. g., 10-mer peptides were bypassed, while 23-mers were not) (70,71,73). In another report, even a large 31-mer peptide conjugated to 5-formylcytosine was bypassed by translesion DNA polymerases κ and η (68). Similarly, conjugates through position

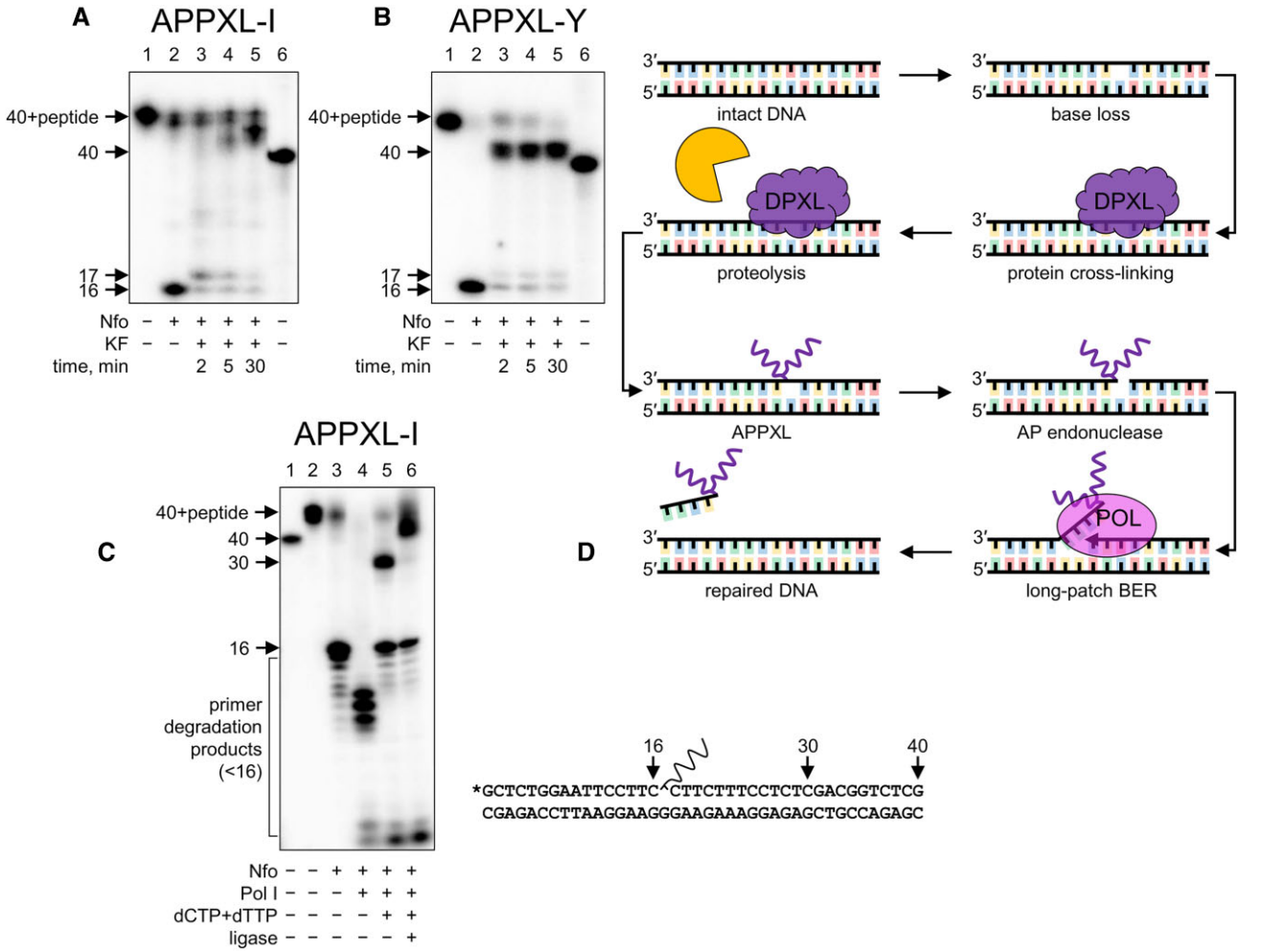

Figure 7. Base excision repair continuation after the cleavage of AP site–peptide cross-links. (A, B) Extension by KF of the primer with the displacement of the downstream strand bearing a 5′-terminal cross-link after Nfo cleavage of APPXL-I (**A**) and APPXL-Y (**B**). Lane 1, cross-linked strand; lane 2, APPXL treated with Nfo; lanes 3–5, APPXL treated with Nfo followed by KF extension for the indicated time; lane 6, size marker corresponding to the unmodified strand. (**C**) Reconstitution of the full BER cycle of APPXL-I with Nfo, Pol I, and DNA ligase. Lane 1 and 2, unmodified and cross-linked strands, respectively; lane 3, substrate cleaved by Nfo; lane 4, substrate cleaved by Nfo in the presence of Pol I without dNTPs; lane 5; substrate cleaved by Nfo and extended by Pol I; lane 6, substrate cleaved by Nfo, extended by Pol I and ligated. (**D**) General scheme of possible BER-dependent repair of AP site–peptide cross-links.

C7 of 7-deazaG are bypassed by translesion polymerases in a size-dependent manner (74). Peptides adducted through the exocyclic amino group of A, which may either eliminate or keep base pairing depending on the orientation of the peptide, completely block *E. coli* replicative DNA polymerase III but demonstrate low-to-full bypass by *E. coli* DNA polymerases I, II, IV and V, human translesion DNA polymerases η, ι, κ and ν, and replicative yeast DNA polymerase δ (65–67). On the other hand, peptide adducts with the exocyclic group of G, which either disrupt base pairing or protrude into the minor groove, are strongly blocking for most polymerases and were efficiently bypassed only by Family Y translesion DNA polymerases (*E. coli* Pol IV and human Pol κ) (64,65). In the cell, mutagenic bypass of peptide adducts requires translesion DNA polymerases (69,70,75).

Bypass of natural AP sites and their modified varieties is often described by the 'A-rule', which states that dAMP insertion is preferred opposite a non-instructive lesion. Interestingly, the structural reasons underlying this preference are different between DNA polymerases. For example, the structure of the Stoffel fragment of Taq DNA polymerase (which corresponds to KF in the *E. coli* enzyme) shows templating by a conservative Tyr residue inserted in place of a template nucleotide and acting as a thymine mimic (76,77). RBpol, on the other hand, relies on the favorable stacking between the incoming dATP and the extended planar system formed by the terminal primer nucleotide and its pairing partner in the absence of the template nucleobase (78,79). However, in the structures of both polymerases with AP-DNA, C1′ of the AP site resides is buried at the protein–DNA interface, and the template strand would require extensive conformational rearrangement for a bypass if a large peptide is attached to this position. The steric clash could be relieved by flipping the template nucleotide around its flanking phosphates, as often observed in

structures of Families X and Y DNA polymerases stabilizing a misaligned primer–template junction (80–82). In the 'open' state of the enzyme–DNA complex, Family A DNA polymerases, including KF, also rotate the downstream template nucleotides outside of the helix, and it has been suggested that this movement helps prevent the template bases from misalignment in the absence of an incoming dNTP (83). As we do not see preferential incorporation of a dNMP corresponding to +1 template nucleotide, characteristic of the primer–template misalignment bypass mechanism, we hypothesize that favorable stacking can guide dAMP and dGMP insertion opposite extrahelical APPXLs in the rare bypass events. On the other hand, structures of Dpo4 bypassing an abasic site, demonstrate extensive conformational flexibility allowing for primer/template misalignment and generation of mismatches, +1 and −1 frameshifts (84). In the structure with misalignment between the primer end and the +1 position in the template (which was observed in our experiments), the AP site is looped out of the helix into a gap between the fingers and the little finger domains, providing plenty of space for accommodation of a cross-linked peptide. No structure of PolX in the frameshift mode is available but POLβ, a prototypical member of Family X, can also loop out a template nucleotide to match the primer end to the +1 position in the template (82).

As we used representative DNA polymerases of non-human origin in our study, it remains to be seen which DNA polymerases may participate in APPXL bypass in human cells. Based on the *in vitro* insertion specificity data, it has long been held that natural AP sites are bypassed by DNA polymerase η (POLη) (85,86). On the other hand, AP site bypass in POLη-deficient human cells is almost as efficient as in wild-type cells (87). An alternative model was proposed, based on yeast mutation spectra and *in vitro* biochemistry of human and yeast DNA polymerase ζ (POLζ), that the POLζ/REV1 complex acting both as an inserter and an extender polymerase provides mutagenic bypass of AP sites (reviewed in (88)). However, mutation spectra induced by AP sites in yeast and human cells seem to be different (89), and human REV1 also interacts with DNA polymerases η, κ and ι (88), so the nature of the inserter polymerase in human cells exposed to AP sites or their derivatives, including APPXLs, needs further investigation.

The high proficiency of TIM barrel AP endonucleases in nicking DNA at APPXLs was rather unexpected, since even the known substrates for the NIR activity of these enzymes are much less bulky. However, inspection of the structures of DNA-bound Nfo (90,91) reveals that C1′ is solvent-accessible in both enzyme–substrate and enzyme–product complexes (Supplementary Figure S8) and the attached peptide could possibly be accommodated in the major groove of the DNA molecule, which is sharply bent upon Nfo binding. The structure of yeast Apn1p has not been solved but a similar C1′ exposure is observed in a DNA-bound African swine fever virus AP endonuclease (92), another TIM barrel superfamily member. At the same time, the C1′ atom of the target nucleotide is fully buried in the complex of APE1 with AP site-containing DNA, the nicked AP product, or 3′-terminal mismatched dNMPs that are substrates for the exonuclease activity of APE1 (93–95). The structure of DNA-bound *E. coli* Xth is not available but in the structurally related AP endonuclease from *Neisseria meningitidis* the C1′ atom is also inaccessible (96). Thus, structural reasons may explain the lack of cleavage of the APPXL substrates by Xth and the mediocre cleavage by APE1 despite its NIR activity being capable of processing bulky etheno adducts (59,62). The remaining activity of APE1 on APPXL-Y may be due to a more pronounced duplex destabilization by the larger peptide, which would make easier the access to the phosphate of the damaged nucleotide without fully moving the peptide part into the AP site-recognition pocket.

Overall, our results suggest that, at least in bacteria and budding yeast, APPXL may be repaired by the BER pathway. After the initial nick by Nfo/Apn1p, the repair could proceed along the long-patch branch displacing or degrading a flap decorated with the 5′-terminal adduct. Alternatively, it is possible that 2′-deoxyribo-5′-phosphate lyases, such as RecJ or Fpg in *E. coli* (97,98) and Trf4 in yeast (99), or exonucleases resolving topoisomerase II-type adducts (100,101), can catalyze excision of 5′-terminal imine-peptide AP adducts, or that such conjugates undergo spontaneous β-elimination (102,103), allowing the repair to continue through the short-patch subpathway. As for human cells, given that under NIR conditions APE1 processed APPXL-Y and OHU at about the same order of magnitude, BER could also contribute, at least partly, to APPXL repair. Possible alternatives include NER (104,105), homologous recombination (106), or direct adduct uncoupling by HMCES-SRAP proteins (107). Interestingly, Nfo/Apn1p homologs are present in fish and amphibians, raising a possibility that BER of APPXL may be evolutionarily conserved and occur even in vertebrates.

DATA AVAILABILITY

All data are provided in the paper and the supplementary materials.

SUPPLEMENTARY DATA

Supplementary Data are available at NAR Online.

ACKNOWLEDGEMENTS

Mass spectrometry was performed at the SB RAS Institute of Chemical Biology and Fundamental Medicine Joint Center for Genomic, Proteomic and Metabolomics Studies. We thank Dr Alexander A. Chernonosov for helpful discussion.

FUNDING

Russian Science Foundation [21-74-00061 to A.V.Y., all biochemical experiments]; Fondation ARC [PJA-2021060003796 to A.A.I.]; Russian Ministry of Higher Education and Science [121031300056-8 to D.O.Z.]; D.V.K. is supported by a graduate student fellowship from the Russian Foundation for Basic Research [20-34-90092]. Funding for open access charge: SB RAS ICBFM intramural program.

Conflict of interest statement. None declared.

REFERENCES

1. Lindahl,T. and Nyberg,B. (1972) Rate of depurination of native deoxyribonucleic acid. *Biochemistry*, **11**, 3610–3618.
2. Atamna,H., Cheung,I. and Ames,B.N. (2000) A method for detecting abasic sites in living cells: age-dependent changes in base excision repair. *Proc. Natl Acad. Sci. U.S.A.*, **97**, 686–691.
3. Boiteux,S. and Guillet,M. (2004) Abasic sites in DNA: repair and biological consequences in *Saccharomyces cerevisiae*. *DNA Repair (Amst.)*, **3**, 1–12.
4. Thompson,P.S. and Cortez,D. (2020) New insights into abasic site repair and tolerance. *DNA Repair (Amst.)*, **90**, 102866.
5. DeMott,M.S., Beyret,E., Wong,D., Bales,B.C., Hwang,J.-T., Greenberg,M.M. and Demple,B. (2002) Covalent trapping of human DNA polymerase β by the oxidative DNA lesion 2-deoxyribonolactone. *J. Biol. Chem.*, **277**, 7637–7640.
6. Sczepanski,J.T., Wong,R.S., McKnight,J.N., Bowman,G.D. and Greenberg,M.M. (2010) Rapid DNA–protein cross-linking and strand scission by an abasic site in a nucleosome core particle. *Proc. Natl Acad. Sci. U.S.A.*, **107**, 22475–22480.
7. Greenberg,M.M. (2014) Abasic and oxidized abasic site reactivity in DNA: enzyme inhibition, cross-linking, and nucleosome catalyzed reactions. *Acc. Chem. Res.*, **47**, 646–655.
8. Greenberg,M.M., Weledji,Y.N., Kroeger,K.M. and Kim,J. (2004) In vitro replication and repair of DNA containing a C2′-oxidized abasic site. *Biochemistry*, **43**, 15217–15222.
9. Guan,L. and Greenberg,M.M. (2009) DNA interstrand cross-link formation by the 1,4-dioxobutane abasic lesion. *J. Am. Chem. Soc.*, **131**, 15225–15231.
10. Ghosh,S. and Greenberg,M.M. (2015) Correlation of thermal stability and structural distortion of DNA interstrand cross-links produced from oxidized abasic sites with their selective formation and repair. *Biochemistry*, **54**, 6274–6283.
11. Fortini,P. and Dogliotti,E. (2007) Base damage and single-strand break repair: mechanisms and functional significance of short- and long-patch repair subpathways. *DNA Repair (Amst.)*, **6**, 398–409.
12. Wong,R.S., Sczepanski,J.T. and Greenberg,M.M. (2010) Excision of a lyase-resistant oxidized abasic lesion from DNA. *Chem. Res. Toxicol.*, **23**, 766–770.
13. Hashimoto,M., Greenberg,M.M., Kow,Y.W., Hwang,J.-T. and Cunningham,R.P. (2001) The 2-deoxyribonolactone lesion produced in DNA by neocarzinostatin and other damaging agents forms cross-links with the base-excision repair enzyme endonuclease III. *J. Am. Chem. Soc.*, **123**, 3161–3162.
14. Kroeger,K.M., Hashimoto,M., Kow,Y.W. and Greenberg,M.M. (2003) Cross-linking of 2-deoxyribonolactone and its β-elimination product by base excision repair enzymes. *Biochemistry*, **42**, 2449–2455.
15. Guan,L. and Greenberg,M.M. (2010) Irreversible inhibition of DNA polymerase β by an oxidized abasic lesion. *J. Am. Chem. Soc.*, **132**, 5004–5005.
16. Guan,L., Bebenek,K., Kunkel,T.A. and Greenberg,M.M. (2010) Inhibition of short patch and long patch base excision repair by an oxidized abasic site. *Biochemistry*, **49**, 9904–9910.
17. Sczepanski,J.T., Zhou,C. and Greenberg,M.M. (2013) Nucleosome core particle-catalyzed strand scission at abasic sites. *Biochemistry*, **52**, 2157–2164.
18. Ren,M., Shang,M., Wang,H., Xi,Z. and Zhou,C. (2021) Histones participate in base excision repair of 8-oxodGuo by transiently cross-linking with active repair intermediates in nucleosome core particles. *Nucleic Acids Res.*, **49**, 257–268.
19. Mazumder,A., Neamati,N., Pilon,A.A., Sunder,S. and Pommier,Y. (1996) Chemical trapping of ternary complexes of human immunodeficiency virus type 1 integrase, divalent metal, and DNA substrates containing an abasic site: implications for the role of lysine 136 in DNA binding. *J. Biol. Chem.*, **271**, 27330–27338.
20. Bogenhagen,D.F. and Pinz,K.G. (1998) The action of DNA ligase at abasic sites in DNA. *J. Biol. Chem.*, **273**, 7888–7893.
21. Kosova,A.A., Khodyreva,S.N. and Lavrik,O.I. (2016) Ku antigen displays the AP lyase activity on a certain type of duplex DNA. *Biochim. Biophys. Acta*, **1864**, 1244–1252.
22. Rieger,R.A., Zaika,E.I., Xie,W., Johnson,F., Grollman,A.P., Iden,C.R. and Zharkov,D.O. (2006) Proteomic approach to identification of proteins reactive for abasic sites in DNA. *Mol. Cell. Proteomics*, **5**, 858–867.
23. Grosheva,A.S., Zharkov,D.O., Stahl,J., Gopanenko,A.V., Tupikin,A.E., Kabilov,M.R., Graifer,D.M. and Karpova,G.G. (2017) Recognition but no repair of abasic site in single-stranded DNA by human ribosomal uS3 protein residing within intact 40S subunit. *Nucleic Acids Res.*, **45**, 3833–3843.
24. Kosova,A.A., Khodyreva,S.N. and Lavrik,O.I. (2015) Glyceraldehyde-3-phosphate dehydrogenase (GAPDH) interacts with apurinic/apyrimidinic sites in DNA. *Mutat. Res.*, **779**, 46–57.
25. Halabelian,L., Ravichandran,M., Li,Y., Zeng,H., Rao,A., Aravind,L. and Arrowsmith,C.H. (2019) Structural basis of HMCES interactions with abasic DNA and multivalent substrate recognition. *Nat. Struct. Mol. Biol.*, **26**, 607–612.
26. Mohni,K.N., Wessel,S.R., Zhao,R., Wojciechowski,A.C., Luzwick,J.W., Layden,H., Eichman,B.F., Thompson,P.S., Mehta,K.P.M. and Cortez,D. (2019) HMCES maintains genome integrity by shielding abasic sites in single-strand DNA. *Cell*, **176**, 144–153.
27. Thompson,P.S., Amidon,K.M., Mohni,K.N., Cortez,D. and Eichman,B.F. (2019) Protection of abasic sites during DNA replication by a stable thiazolidine protein-DNA cross-link. *Nat. Struct. Mol. Biol.*, **26**, 613–618.
28. Barker,S., Weinfeld,M. and Murray,D. (2005) DNA–protein crosslinks: their induction, repair, and biological consequences. *Mutat. Res.*, **589**, 111–135.
29. Pommier,Y., Leo,E., Zhang,H. and Marchand,C. (2010) DNA topoisomerases and their poisoning by anticancer and antibacterial drugs. *Chem. Biol.*, **17**, 421–433.
30. Duxin,J.P., Dewar,J.M., Yardimci,H. and Walter,J.C. (2014) Repair of a DNA-protein crosslink by replication-coupled proteolysis. *Cell*, **159**, 346–357.
31. Stingele,J., Schwarz,M.S., Bloemeke,N., Wolf,P.G. and Jentsch,S. (2014) A DNA-dependent protease involved in DNA-protein crosslink repair. *Cell*, **158**, 327–338.
32. Vaz,B., Popovic,M., Newman,J.A., Fielden,J., Aitkenhead,H., Halder,S., Singh,A.N., Vendrell,I., Fischer,R., Torrecilla,I. *et al.* (2016) Metalloprotease SPRTN/DVC1 orchestrates replication-coupled DNA-protein crosslink repair. *Mol. Cell*, **64**, 704–719.
33. Larsen,N.B., Gao,A.O., Sparks,J.L., Gallina,I., Wu,R.A., Mann,M., Räschle,M., Walter,J.C. and Duxin,J.P. (2019) Replication-coupled DNA-protein crosslink repair by SPRTN and the proteasome in *Xenopus* egg extracts. *Mol. Cell*, **73**, 574–588.
34. Quievryn,G. and Zhitkovich,A. (2000) Loss of DNA–protein crosslinks from formaldehyde-exposed cells occurs through spontaneous hydrolysis and an active repair process linked to proteosome function. *Carcinogenesis*, **21**, 1573–1580.
35. Minko,I.G., Kurtz,A.J., Croteau,D.L., Van Houten,B., Harris,T.M. and Lloyd,R.S. (2005) Initiation of repair of DNA–polypeptide cross-links by the UvrABC nuclease. *Biochemistry*, **44**, 3000–3009.
36. Nakano,T., Morishita,S., Katafuchi,A., Matsubara,M., Horikawa,Y., Terato,H., Salem,A.M.H., Izumi,S., Pack,S.P., Makino,K. *et al.* (2007) Nucleotide excision repair and homologous recombination systems commit differentially to the repair of DNA-protein crosslinks. *Mol. Cell*, **28**, 147–158.
37. de Graaf,B., Clore,A. and McCullough,A.K. (2009) Cellular pathways for DNA repair and damage tolerance of formaldehyde-induced DNA-protein crosslinks. *DNA Repair (Amst.)*, **8**, 1207–1214.
38. McKibbin,P.L., Fleming,A.M., Towheed,M.A., Van Houten,B., Burrows,C.J. and David,S.S. (2013) Repair of hydantoin lesions and their amine adducts in DNA by base and nucleotide excision repair. *J. Am. Chem. Soc.*, **135**, 13851–13861.
39. Gilboa,R., Zharkov,D.O., Golan,G., Fernandes,A.S., Gerchman,S.E., Matz,E., Kycia,J.H., Grollman,A.P. and Shoham,G. (2002) Structure of formamidopyrimidine-DNA glycosylase covalently complexed to DNA. *J. Biol. Chem.*, **277**, 19811–19816.
40. Rieger,R.A., McTigue,M.M., Kycia,J.H., Gerchman,S.E., Grollman,A.P. and Iden,C.R. (2000) Characterization of a cross-linked DNA-endonuclease VIII repair complex by electrospray

ionization mass spectrometry. *J. Am. Soc. Mass Spectrom.*, **11**, 505–515.
41. Ishchenko,A.A., Sanz,G., Privezentzev,C.V., Maksimenko,A.V. and Saparbaev,M. (2003) Characterisation of new substrate specificities of *Escherichia coli* and *Saccharomyces cerevisiae* AP endonucleases. *Nucleic Acids Res.*, **31**, 6344–6353.
42. Sidorenko,V.S., Nevinsky,G.A. and Zharkov,D.O. (2007) Mechanism of interaction between human 8-oxoguanine-DNA glycosylase and AP endonuclease. *DNA Repair (Amst.)*, **6**, 317–328.
43. Kuznetsov,N.A., Koval,V.V., Zharkov,D.O., Nevinsky,G.A., Douglas,K.T. and Fedorova,O.S. (2005) Kinetics of substrate recognition and cleavage by human 8-oxoguanine-DNA glycosylase. *Nucleic Acids Res.*, **33**, 3919–3931.
44. Katafuchi,A., Nakano,T., Masaoka,A., Terato,H., Iwai,S., Hanaoka,F. and Ide,H. (2004) Differential specificity of human and *Escherichia coli* endonuclease III and VIII homologues for oxidative base lesions. *J. Biol. Chem.*, **279**, 14464–14471.
45. Kakhkharova,Z.I., Zharkov,D.O. and Grin,I.R. (2022) A low-activity polymorphic variant of human NEIL2 DNA glycosylase. *Int. J. Mol. Sci.*, **23**, 2212.
46. Miller,H. and Grollman,A.P. (1997) Kinetics of DNA polymerase I (Klenow fragment exo$^-$) activity on damaged DNA templates: effect of proximal and distal template damage on DNA synthesis. *Biochemistry*, **36**, 15336–15342.
47. Freisinger,E., Grollman,A.P., Miller,H. and Kisker,C. (2004) Lesion (in)tolerance reveals insights into DNA replication fidelity. *EMBO J.*, **23**, 1494–1505.
48. Yudkina,A.V., Dvornikova,A.P. and Zharkov,D.O. (2018) Variable termination sites of DNA polymerases encountering a DNA–protein cross-link. *PLoS One*, **13**, e0198480.
49. Boldinova,E.O., Yudkina,A.V., Shilkin,E.S., Gagarinskaya,D.I., Baranovskiy,A.G., Tahirov,T.H., Zharkov,D.O. and Makarova,A.V. (2021) Translesion activity of PrimPol on DNA with cisplatin and DNA–protein cross-links. *Sci. Rep.*, **11**, 17588.
50. Yudkina,A.V., Shilkin,E.S., Makarova,A.V. and Zharkov,D.O. (2022) Stalling of eukaryotic translesion DNA polymerases at DNA-protein cross-links. *Genes*, **13**, 166.
51. Fromme,J.C., Bruner,S.D., Yang,W., Karplus,M. and Verdine,G.L. (2003) Product-assisted catalysis in base-excision DNA repair. *Nat. Struct. Biol.*, **10**, 204–211.
52. Kumar,S., Lamarche,B.J. and Tsai,M.-D. (2007) Use of damaged DNA and dNTP substrates by the error-prone DNA polymerase X from african swine fever virus. *Biochemistry*, **46**, 3814–3825.
53. Howard,M.J. and Wilson,S.H. (2018) DNA scanning by base excision repair enzymes and implications for pathway coordination. *DNA Repair (Amst.)*, **71**, 101–107.
54. Goodman,M.F., Cai,H., Bloom,L.B. and Eritja,R. (1994) Nucleotide insertion and primer extension at abasic template sites in different sequence contexts. *Ann. N. Y. Acad. Sci.*, **726**, 132–142.
55. Paz-Elizur,T., Takeshita,M. and Livneh,Z. (1997) Mechanism of bypass synthesis through an abasic site analog by DNA polymerase I. *Biochemistry*, **36**, 1766–1773.
56. Taylor,J.-S. (2002) New structural and mechanistic insight into the A-rule and the instructional and non-instructional behavior of DNA photoproducts and other lesions. *Mutat. Res.*, **510**, 55–70.
57. Kokoska,R.J., Bebenek,K., Boudsocq,F., Woodgate,R. and Kunkel,T.A. (2002) Low fidelity DNA synthesis by a y family DNA polymerase due to misalignment in the active site. *J. Biol. Chem.*, **277**, 19633–19638.
58. Ide,H., Tedzuka,K., Shimzu,H., Kimura,Y., Purmal,A.A., Wallace,S.S. and Kow,Y.W. (1994) α-Deoxyadenosine, a major anoxic radiolysis product of adenine in DNA, is a substrate for *Escherichia coli* endonuclease IV. *Biochemistry*, **33**, 7842–7847.
59. Hang,B., Chenna,A., Fraenkel-Conrat,H. and Singer,B. (1996) An unusual mechanism for the major human apurinic/apyrimidinic (AP) endonuclease involving 5′ cleavage of DNA containing a benzene-derived exocyclic adduct in the absence of an AP site. *Proc. Natl Acad. Sci. U.S.A.*, **93**, 13737–13741.
60. Ischenko,A.A. and Saparbaev,M.K. (2002) Alternative nucleotide incision repair pathway for oxidative DNA damage. *Nature*, **415**, 183–187.
61. Gros,L., Ishchenko,A.A., Ide,H., Elder,R.H. and Saparbaev,M.K. (2004) The major human AP endonuclease (Ape1) is involved in the nucleotide incision repair pathway. *Nucleic Acids Res.*, **32**, 73–81.
62. Prorok,P., Saint-Pierre,C., Gasparutto,D., Fedorova,O.S., Ishchenko,A.A., Leh,H., Buckle,M., Tudek,B. and Saparbaev,M. (2012) Highly mutagenic exocyclic DNA adducts are substrates for the human nucleotide incision repair pathway. *PLoS One*, **7**, e51776.
63. Lyamichev,V., Brow,M.A.D. and Dahlberg,J.E. (1993) Structure-specific endonucleolytic cleavage of nucleic acids by eubacterial DNA polymerases. *Science*, **260**, 778–783.
64. Minko,I.G., Yamanaka,K., Kozekov,I.D., Kozekova,A., Indiani,C., O'Donnell,M.E., Jiang,Q., Goodman,M.F., Rizzo,C.J. and Lloyd,R.S. (2008) Replication bypass of the acrolein-mediated deoxyguanine DNA-peptide cross-links by DNA polymerases of the DinB family. *Chem. Res. Toxicol.*, **21**, 1983–1990.
65. Yamanaka,K., Minko,I.G., Takata,K.-i., Kolbanovskiy,A., Kozekov,I.D., Wood,R.D., Rizzo,C.J. and Lloyd,R.S. (2010) Novel enzymatic function of DNA polymerase *ν* in translesion DNA synthesis past major groove DNA−peptide and DNA−DNA cross-links. *Chem. Res. Toxicol.*, **23**, 689–695.
66. Yamanaka,K., Minko,I.G., Finkel,S.E., Goodman,M.F. and Lloyd,R.S. (2011) Role of high-fidelity *Escherichia coli* DNA polymerase I in replication bypass of a deoxyadenosine DNA-peptide cross-link. *J. Bacteriol.*, **193**, 3815–3821.
67. Ghodke,P.P., Gonzalez-Vasquez,G., Wang,H., Johnson,K.M., Sedgeman,C.A. and Guengerich,F.P. (2021) Enzymatic bypass of an N^6-deoxyadenosine DNA-ethylene dibromide-peptide crosslink by translesion DNA polymerases. *J. Biol. Chem.*, **296**, 100444.
68. Ji,S., Fu,I., Naldiga,S., Shao,H., Basu,A.K., Broyde,S. and Tretyakova,N.Y. (2018) 5-Formylcytosine mediated DNA–protein cross-links block DNA replication and induce mutations in human cells. *Nucleic Acids Res.*, **46**, 6455–6469.
69. Ji,S., Park,D., Kropachev,K., Essawy,M., Geacintov,N.E. and Tretyakova,N.Y. (2019) 5-Formylcytosine-induced DNA–peptide cross-links reduce transcription efficiency, but do not cause transcription errors in human cells. *J. Biol. Chem.*, **294**, 18387–18397.
70. Naldiga,S., Ji,S., Thomforde,J., Nicolae,C.M., Lee,M., Zhang,Z., Moldovan,G.-L., Tretyakova,N.Y. and Basu,A.K. (2019) Error-prone replication of a 5-formylcytosine-mediated DNA-peptide cross-link in human cells. *J. Biol. Chem.*, **294**, 10619–10627.
71. Wickramaratne,S., Boldry,E.J., Buehler,C., Wang,Y.-C., Distefano,M.D. and Tretyakova,N.Y. (2015) Error-prone translesion synthesis past DNA-peptide cross-links conjugated to the major groove of DNA via C5 of thymidine. *J. Biol. Chem.*, **290**, 775–787.
72. Pande,P., Ji,S., Mukherjee,S., Schärer,O.D., Tretyakova,N.Y. and Basu,A.K. (2017) Mutagenicity of a model DNA-peptide cross-link in human cells: roles of translesion synthesis DNA polymerases. *Chem. Res. Toxicol.*, **30**, 669–677.
73. Yeo,J.E., Wickramaratne,S., Khatwani,S., Wang,Y.-C., Vervacke,J., Distefano,M.D. and Tretyakova,N.Y. (2014) Synthesis of site-specific DNA–protein conjugates and their effects on DNA replication. *ACS Chem. Biol.*, **9**, 1860–1868.
74. Wickramaratne,S., Ji,S., Mukherjee,S., Su,Y., Pence,M.G., Lior-Hoffmann,L., Fu,I., Broyde,S., Guengerich,F.P., Distefano,M. *et al.* (2016) Bypass of DNA-protein cross-links conjugated to the 7-deazaguanine position of DNA by translesion synthesis polymerases. *J. Biol. Chem.*, **291**, 23589–23603.
75. Ji,S., Thomforde,J., Rogers,C., Fu,I., Broyde,S. and Tretyakova,N.Y. (2019) Transcriptional bypass of DNA–protein and DNA–peptide conjugates by T7 RNA polymerase. *ACS Chem. Biol.*, **14**, 2564–2575.
76. Obeid,S., Blatter,N., Kranaster,R., Schnur,A., Diederichs,K., Welte,W. and Marx,A. (2010) Replication through an abasic DNA lesion: structural basis for adenine selectivity. *EMBO J.*, **29**, 1738–1747.
77. Obeid,S., Welte,W., Diederichs,K. and Marx,A. (2012) Amino acid templating mechanisms in selection of nucleotides opposite abasic sites by a family A DNA polymerase. *J. Biol. Chem.*, **287**, 14099–14108.
78. Zahn,K.E., Belrhali,H., Wallace,S.S. and Doublié,S. (2007) Caught bending the A-rule: crystal structures of translesion DNA synthesis with a non-natural nucleotide. *Biochemistry*, **46**, 10551–10561.
79. Xia,S., Vashishtha,A., Bulkley,D., Eom,S.H., Wang,J. and Konigsberg,W.H. (2012) Contribution of partial charge interactions

and base stacking to the efficiency of primer extension at and beyond abasic sites in DNA. *Biochemistry*, **51**, 4922–4931.
80. Garcia-Diaz,M., Bebenek,K., Krahn,J.M., Pedersen,L.C. and Kunkel,T.A. (2006) Structural analysis of strand misalignment during DNA synthesis by a human DNA polymerase. *Cell*, **124**, 331–342.
81. Bauer,J., Xing,G., Yagi,H., Sayer,J.M., Jerina,D.M. and Ling,H. (2007) A structural gap in Dpo4 supports mutagenic bypass of a major benzo[*a*]pyrene dG adduct in DNA through template misalignment. *Proc. Natl Acad. Sci. U.S.A.*, **104**, 14905–14910.
82. Howard,M.J., Cavanaugh,N.A., Batra,V.K., Shock,D.D., Beard,W.A. and Wilson,S.H. (2020) DNA polymerase β nucleotide-stabilized template misalignment fidelity depends on local sequence context. *J. Biol. Chem.*, **295**, 529–538.
83. Patel,P.H., Suzuki,M., Adman,E., Shinkai,A. and Loeb,L.A. (2001) Prokaryotic DNA polymerase I: evolution, structure, and "base flipping" mechanism for nucleotide selection. *J. Mol. Biol.*, **308**, 823–837.
84. Ling,H., Boudsocq,F., Woodgate,R. and Yang,W. (2004) Snapshots of replication through an abasic lesion: structural basis for base substitutions and frameshifts. *Mol. Cell*, **13**, 751–762.
85. Zhang,Y., Yuan,F., Wu,X., Rechkoblit,O., Taylor,J.-S., Geacintov,N.E. and Wang,Z. (2000) Error-prone lesion bypass by human DNA polymerase η. *Nucleic Acids Res.*, **28**, 4717–4724.
86. Choi,J.-Y., Lim,S., Kim,E.-J., Jo,A. and Guengerich,F.P. (2010) Translesion synthesis across abasic lesions by human B-family and Y-family DNA polymerases α, δ, η, ι, κ, and REV1. *J. Mol. Biol.*, **404**, 34–44.
87. Avkin,S., Adar,S., Blander,G. and Livneh,Z. (2002) Quantitative measurement of translesion replication in human cells: evidence for bypass of abasic sites by a replicative DNA polymerase. *Proc. Natl Acad. Sci. U.S.A.*, **99**, 3764–3769.
88. Makarova,A.V. and Burgers,P.M. (2015) Eukaryotic DNA polymerase ζ. *DNA Repair (Amst.)*, **29**, 47–55.
89. Weerasooriya,S., Jasti,V.P. and Basu,A.K. (2014) Replicative bypass of abasic site in *Escherichia coli* and human cells: similarities and differences. *PLoS One*, **9**, e107915.
90. Hosfield,D.J., Guan,Y., Haas,B.J., Cunningham,R.P. and Tainer,J.A. (1999) Structure of the DNA repair enzyme endonuclease IV and its DNA complex: double-nucleotide flipping at abasic sites and three-metal-ion catalysis. *Cell*, **98**, 397–408.
91. Garcin,E.D., Hosfield,D.J., Desai,S.A., Haas,B.J., Björas,M., Cunningham,R.P. and Tainer,J.A. (2008) DNA apurinic-apyrimidinic site binding and excision by endonuclease IV. *Nat. Struct. Mol. Biol.*, **15**, 515–522.
92. Chen,Y., Chen,X., Huang,Q., Shao,Z., Gao,Y., Li,Y., Yang,C., Liu,H., Li,J., Wang,Q. *et al.* (2020) A unique DNA-binding mode of African swine fever virus AP endonuclease. *Cell Discov.*, **6**, 13.
93. Mol,C.D., Izumi,T., Mitra,S. and Tainer,J.A. (2000) DNA-bound structures and mutants reveal abasic DNA binding by APE1 and DNA repair coordination. *Nature*, **403**, 451–456.
94. Freudenthal,B.D., Beard,W.A., Cuneo,M.J., Dyrkheeva,N.S. and Wilson,S.H. (2015) Capturing snapshots of APE1 processing DNA damage. *Nat. Struct. Mol. Biol.*, **22**, 924–931.
95. Whitaker,A.M., Flynn,T.S. and Freudenthal,B.D. (2018) Molecular snapshots of APE1 proofreading mismatches and removing DNA damage. *Nat. Commun.*, **9**, 399.
96. Lu,D., Silhan,J., MacDonald,J.T., Carpenter,E.P., Jensen,K., Tang,C.M., Baldwin,G.S. and Freemont,P.S. (2012) Structural basis for the recognition and cleavage of abasic DNA in *Neisseria meningitidis*. *Proc. Natl Acad. Sci. U.S.A.*, **109**, 16852–16857.
97. Graves,R.J., Felzenszwalb,I., Laval,J. and O'Connor,T.R. (1992) Excision of 5′-terminal deoxyribose phosphate from damaged DNA is catalyzed by the Fpg protein of *Escherichia coli*. *J. Biol. Chem.*, **267**, 14429–14435.
98. Dianov,G., Sedgwick,B., Daly,G., Olsson,M., Lovett,S. and Lindahl,T. (1994) Release of 5′-terminal deoxyribose-phosphate residues from incised abasic sites in DNA by the *Escherichia coli* RecJ protein. *Nucleic Acids Res.*, **22**, 993–998.
99. Gellon,L., Carson,D.R., Carson,J.P. and Demple,B. (2008) Intrinsic 5′-deoxyribose-5-phosphate lyase activity in *Saccharomyces cerevisiae* Trf4 protein with a possible role in base excision DNA repair. *DNA Repair (Amst.)*, **7**, 187–198.
100. Neale,M.J., Pan,J. and Keeney,S. (2005) Endonucleolytic processing of covalent protein-linked DNA double-strand breaks. *Nature*, **436**, 1053–1057.
101. Huang,S.-Y.N., Michaels,S.A., Mitchell,B.B., Majdalani,N., Vanden Broeck,A., Canela,A., Tse-Dinh,Y.-C., Lamour,V. and Pommier,Y. (2021) Exonuclease VII repairs quinolone-induced damage by resolving DNA gyrase cleavage complexes. *Sci. Adv.*, **7**, eabe0384.
102. Jha,J.S., Nel,C., Haldar,T., Peters,D., Housh,K. and Gates,K.S. (2022) Products generated by amine-catalyzed strand cleavage at apurinic/apyrimidinic sites in DNA: new insights from a biomimetic nucleoside model system. *Chem. Res. Toxicol.*, **35**, 203–217.
103. Haldar,T., Jha,J.S., Yang,Z., Nel,C., Housh,K., Cassidy,O.J. and Gates,K.S. (2022) Unexpected complexity in the products arising from NaOH-, heat-, amine-, and glycosylase-induced strand cleavage at an abasic site in DNA. *Chem. Res. Toxicol.*, **35**, 218–232.
104. Reardon,J.T. and Sancar,A. (2006) Repair of DNA–polypeptide crosslinks by human excision nuclease. *Proc. Natl Acad. Sci. U.S.A.*, **103**, 4056–4061.
105. Baker,D.J., Wuenschell,G., Xia,L., Termini,J., Bates,S.E., Riggs,A.D. and O'Connor,T.R. (2007) Nucleotide excision repair eliminates unique DNA-protein cross-links from mammalian cells. *J. Biol. Chem.*, **282**, 22592–22604.
106. Nakano,T., Katafuchi,A., Matsubara,M., Terato,H., Tsuboi,T., Masuda,T., Tatsumoto,T., Pack,S.P., Makino,K., Croteau,D.L. *et al.* (2009) Homologous recombination but not nucleotide excision repair plays a pivotal role in tolerance of DNA-protein cross-links in mammalian cells. *J. Biol. Chem.*, **284**, 27065–27076.
107. Paulin,K.A., Cortez,D. and Eichman,B.F. (2022) The SOS response-associated peptidase (SRAP) domain of YedK catalyzes ring opening of abasic sites and reversal of its DNA-protein crosslink. *J. Biol. Chem.*, **298**, 102307.